Science of the Total Environment 823 (2022) 153587

Contents lists available at ScienceDirect

Science of the Total Environment

journal homepage: www.elsevier.com/locate/scitotenv

Can ecological landscape pattern influence dry-wet dynamics? A national scale assessment in China from 1980 to 2018

Yang Han [a], Di Chang [b], Xiao-zhi Xiang [c], Jing-lei Wang [a,*]

[a] Farmland Irrigation Research Institute, Chinese Academy of Agricultural Sciences, Xinxiang 453002, China.
[b] Key Laboratory of Virtual Geographic Environment, Nanjing Normal University, Ministry of Education, Nanjing 210023, China.
[c] Institute of Geography and Resources Science, Sichuan Normal University, Chengdu 610066, China.

HIGHLIGHTS

- Response of dry-wet dynamics to landscape pattern was examined.
- Increased abundance in forest and crop landscapes can reduce drought risk.
- Enhanced forest connectivity can optimize dry-wet environment.
- Large-scale grass landscape would increase extreme drought risk.
- Balance between agricultural benefit and crop landscape effect should be considered.

GRAPHICAL ABSTRACT

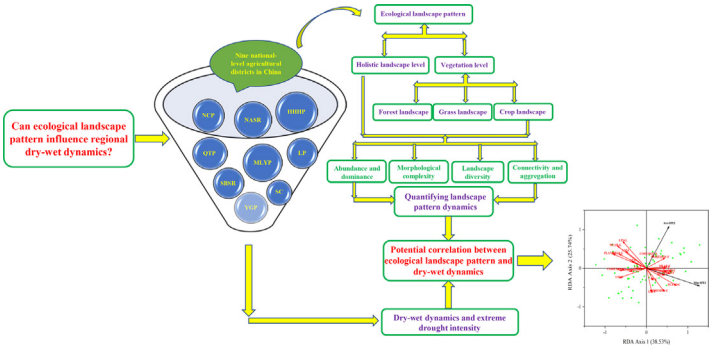

ARTICLE INFO

Article history:
Received 16 November 2021
Received in revised form 25 January 2022
Accepted 28 January 2022
Available online 2 February 2022

Editor: Fernando A.L. Pacheco

Keywords:
Landscape indicators
Vegetation category
Drought
Optimal configuration
National-level agricultural districts

ABSTRACT

Land cover has been demonstrated to have substantial impacts on climate and dry-wet environment, but potential influence of landscape pattern dynamics accompanying land cover change on drought remains unclear. In this study, response of dry-wet dynamics to landscape pattern in China was examined. Results suggest that landscape pattern in China's nine agricultural districts had transformed to varying extents and showed spatiotemporal heterogeneity from 1980 to 2018. For forest landscape, the highest annual average Percentage of Landscape (PLAND) was recorded in SC, reaching 62.26%; and the highest Largest Patch Index (LPI) was presented in YGP, followed by SC, with annual values of 53.79% and 46.26% respectively. The QTP has the most prominent forest connectivity in spite of its lower abundance. For grass landscape, the highest abundance and dominance were recorded in QTP, with annual PLAND fluctuation range of 49.66%—63.52% and annual LPI variation range of 34.10%—58.46%, which is associated with its climate and altitude. The most prominent crop landscape abundance and dominance were recorded in HHHP, with annual PLAND fluctuating interval of 56.53%—60.64%, indicating the highest agricultural development level in this district. At landscape level, dry-wet circumstance could be improved with enhancements in the largest patch percentage, patch density and spatial connectivity, while worsen with increases of landscape fragmentation and separated degree. At class level, increases in abundance and dominance of forest and crop landscapes would reduce drought risk, while it was opposite for grass landscape. Improved forest connectedness would optimize dry-wet environment and reduce drought risk. The PLAND of forest and crop landscapes contributed the most prominent effect to alleviate drought intensity. Compared with forestland and grassland, determining suitable crop landscape configuration to reduce drought risk is more complex because the balance between agricultural economic benefits and ecological landscape effects should be taken into account.

* Corresponding author at: Farmland Irrigation Research Institute, Chinese Academy of Agricultural Sciences, No. 380 Hong-Li Road, Xinxiang, Henan 453002, China.
E-mail address: firiwjl@126.com (J. Wang).

http://dx.doi.org/10.1016/j.scitotenv.2022.153587

1. Introduction

Globally, drought is profoundly threatening sustainable developments in various industries (Lu et al., 2019a, 2019b; Pedro-Monzonís et al., 2015; Wang et al., 2017). Over last decades, drought disasters have been extremely common in a multitude of regions around the world (Spinoni et al., 2019; Wang et al., 2021; Zhu et al., 2021) and have even spread to some humid areas (Mishra and Singh, 2010; Zhou et al., 2020), as result of global warming caused by intensification in human activities (Esfahanian et al., 2017; Yao et al., 2018). According to statistics, quite a few regions throughout the world such as North America (Lu et al., 2019a), European (Spinoni et al., 2015a, 2015b), China (Xu et al., 2015) and East Africa (Gebremeskel et al., 2019) are suffering from drought to varying extents. Moreover, the intensity and frequency of drought are expected to continuously increase in future climate scenarios as pervasive irregularity in precipitation and widespread rising in temperature (Song et al., 2021; Wanders and Wada, 2015). This indicates drought may pose a more profound threat to both human society and eco-environment system in future under current social and environmental progression patterns. Therefore, it is essential to examine some controllable ecological factors associated potentially with dry-wet dynamics in current context of human activity, to offer a potential opportunity to regulate drought from a practical perspective, reducing its negative impacts as far as possible.

The formation and occurrence mechanism of drought is complex, associating with various factors concurrently (Yao et al., 2020). Many ecological processes occurred on land surface such as vegetation evapotranspiration and runoff would interact with regional wet-dry environment (Aguilos et al., 2021; Kyatengerwa et al., 2020; Ma et al., 2021; Wang et al., 2019). In recent years, in addition to the direct effects of climatic factors on drought (Vicente-Serrano et al., 2015; Yang et al., 2020), some indirect effects associated with human activities, especially land use/land cover change, have gradually attracted worldwide attention (Fan et al., 2015; Júnior et al., 2015; Peng et al., 2019). Previous researches have suggested that regional land use transformation driven by human activities and social development would pose substantial impacts on a series of climate variables such as temperature, precipitation and humidity by changing some physical properties in land surface (Betts et al., 2007; Mahmood et al., 2014). Variation of territorial underlying surface caused by land utilization shift such as urban expansion would impact radiation balance and energy exchange in ground-atmosphere system, thus changing near-ground meteorological conditions such as temperature, humidity, precipitation and wind speed (Li et al., 2021; Mohammad Harmay et al., 2021; Son et al., 2020). Such variations in climate factors caused by land cover transformation will further influence regional dry-wet circumstances as dry-wet dynamic is prominently affected and restricted by meteorological conditions (Asadi Zarch et al., 2015; Mishra and Singh, 2010; Vicente-Serrano et al., 2020; Zhu et al., 2021). Therefore, it is reasonable to deduce that land cover change would perform a profound impact on regional wet-dry environment. Up to now, although the substantial contribution of land use to regional climate variability has been confirmed, the relationship between land cover pattern as well as its physical configuration variation accompanying land use transformation and dry-wet dynamics remains unclear. This underlying relation needs to be explored, because it can provide a more concrete accordance for regulating dry-wet environment and reducing drought risk from the path of optimizing land planning and allocation.

The spatial composition and configuration, physical morphology, geographical distribution characteristics and diversity of land patches at regional scale synthetically reflect the dynamics and direction of land use progress driven by human activities, constituting the landscape pattern conjointly (Medeiros et al., 2021; Metzger et al., 2021; Yohannes et al., 2021). Landscape pattern is an integrated manifestation of various effects including geographical process, hydro-meteorological effect, human activities and socioeconomic development (Dadashpoor et al., 2019; Deng et al., 2009). Based on the proved correlations between land cover and regional climate as well as dry-wet conditions as mentioned above, it is not difficult to ratiocinate that landscape pattern evolution accompanied by land cover change would constitute a considerable influence on dry-wet dynamics. Furthermore, some researches have demonstrated that landscape pattern change will directly trigger the variations in vegetation cover, hydrological cycling, evapotranspiration and ecological water requirement (Deng et al., 2017; Karlsen et al., 2019; Tordoni et al., 2020; Zhao et al., 2019), and these affected factors are closely correlated with regional dry-wet dynamics (Ding et al., 2020; Jiang et al., 2021; Teuling et al., 2013; Zhao et al., 2015). However, it is still unclear that how landscape pattern impacts dry-wet circumstance, dry-wet dynamic is mainly affected by which concrete landscape indicators, and what is the specific mechanism for such effect.

China, a momentous agricultural country in the world, has been plagued by drought for a long time; and since the reform and opening up, China's land cover and concomitant ecological landscape pattern have undergone drastic transformations. In this study, China was selected as the study area to examine the correlation between landscape pattern and dry-wet dynamics at national-level agricultural division scale. Objectives of this study are as follows: (1) To quantify the variations in ecological landscape pattern, respectively at the holistic landscape level and subordinate vegetation level, among China's nine national-level agricultural districts from 1980 to 2018 using different landscape indicators; (2) to ascertain spatiotemporal variation in dry-wet dynamics using the Standardized Precipitation Evapotranspiration Index (SPEI) across different agricultural districts; and (3) to reveal the impact of landscape pattern evolution on wet-dry environment and to propose some suitable suggestions of landscape pattern optimization strategy aiming at improving dry-wet circumstance and reducing extreme drought risk. The results of this research can provide theoretical guidance and scientific basis for rational landscape planning and configuration to optimize regional dry-wet environment.

2. Methodology

2.1. Study region

China is the largest developing country in the world, ranging from latitudes of 3°31′N to 53°33′N and longitudes of 73°29′E to 135°2′E. Considering that China is a typical agricultural producing country persecuted by drought, it is of great significance to investigate drought at the scale of national-level agricultural district. According to the China's nine major agricultural division standard provided by the Resource and Environment Science and Data Center (https://www.resdc.cn/data.aspx?DATAID=275), the whole China can be divided into a total of nine national-level agricultural districts; respectively the Northeast China Plain (NCP), Yunnan-Guizhou Plateau (YGP), Northern arid and semiarid region (NASR), Southern China (SC), Sichuan Basin and surrounding regions (SBSR), Middle-lower Yangtze Plain (MLYP), Qinghai Tibet Plateau (QTP), Loess Plateau (LP) and Huang-Huai-Hai Plain (HHHP) (Fig. 1). There are obvious discrepancies in climate characteristics between various districts. Climate types across China mainly include subtropical monsoon, temperate monsoon, tropical monsoon, temperate continental climate. Precipitation is gradually decreasing from southeast coast to northwest China. Overall, climate and precipitation among different districts across China have prominent spatiotemporal heterogeneity.

2.2. Data sources

Remote sensing image data for the whole China from 1980 to 2018 were obtained from the Chinese multi-period land use and land cover remote sensing monitoring dataset (CNLUCC), which were downloaded from the Resource and Environment Science and Data Center (http://www.resdc.cn/, last accessed on 2020). The CNLUCC was developed by artificial visual interpretation using Landsat remote sensing image data as the main data source. Spatial resolution is 1 km. Land cover in CNLUCC includes six primary categories: cultivated land, forestland, grassland, water area, residential land and unused land. Furthermore, 25 secondary land cover types were included such as paddies, dry farm, shrubland, open

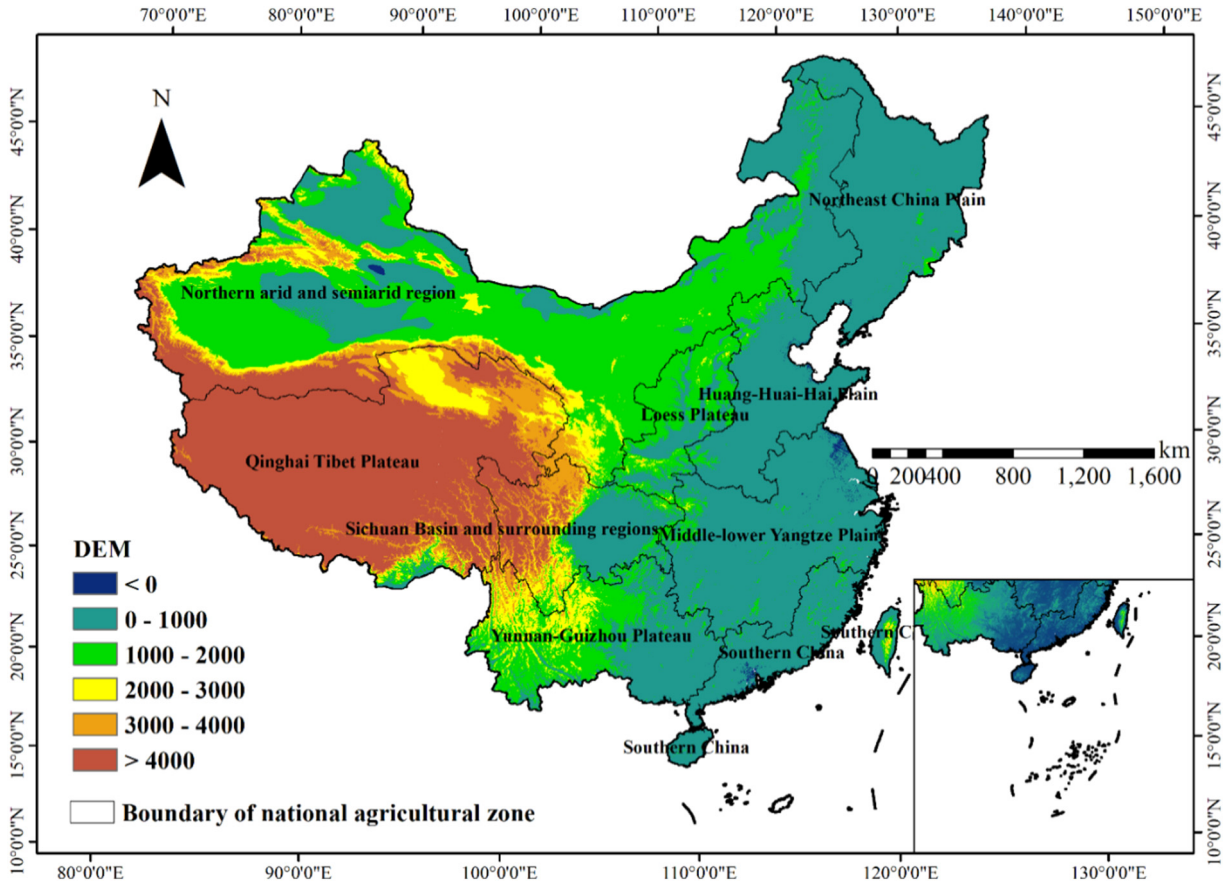

Fig. 1. Study region (Unit of DEM is m).

forestland, high/medium/low density grassland, river and canal, lake, reservoir, intertidal zone, urban land, rural residential land, industrial area and construction land. Meteorological data from 1980 to 2018 were obtained from the China Meteorological Data Sharing Service System (http://data.cma.cn/, last accessed on 2020), the National Tibetan Plateau Science Data Center (http://data.tpdc.ac.cn/zh-hans/, last accessed on 2020) and the Resource and Environment Science and Data Center. In this study, Taiwan, Hong Kong and Macao within the corresponding district were not considered due to the lack of data.

2.3. Landscape pattern analysis

In this research, representative landscape indicators respectively at holistic landscape level and subordinate class level (different vegetation cover types) were investigated to reveal evolution characteristics in ecological landscape pattern among different national-level agricultural districts across China. Landscape indicators at holistic landscape level can reflect various aspects of the variation in landscape structure for a particular region. Indicators at subordinate class level can reflect the dynamic change in landscape pattern of different vegetation cover types within a specified region. Landscape indicators are capable of revealing multiple aspects of ecological landscape configuration, such as spatial distribution, structural complexity, shape characteristics, aggregation, connectedness and diversity. A total of 15 typical landscape indicators involving aspects of area, morphology, spatial distribution and landscape diversity were selected to systematically explore the dynamic variation trend and development direction of landscape patterns. These indicators include the number of patches (NP), patch richness (PR), patch density (PD), mean patch area (MEAR), edge density (ED), percentage of landscape (PLAND), largest patch index (LPI), landscape shape index (LSI), fractal dimension index (FRAC), contiguity index (CONTIG), contagion index (CONTAG), patch cohesion index (COHESION), splitting index (SPLIT), Shannon's diversity index (SHDI) and Simpson's diversity index (SIDI). In present study, FRAGSTATS 4.2 was employed to extract landscape information and to calculate landscape indicators, based on raster data (grids) in remote sensing images (CNLUCC) from 1980 to 2018. Calculation formulas and detailed method descriptions of selected indicators were shown in Table 1.

2.4. Assessment for dry-wet environment

A series of drought indices have been proposed to identify regional dry-wet dynamics, nevertheless, each of them has advantages and disadvantages. For instance, the accuracy of Palmer drought severity index (PDSI) in evaluating short-term drought is insufficient (Guttman, 1998). Although standardized Precipitation Index (SPI) has the advantage of being simple to calculate, it is only suitable for assessing meteorological drought to some extent, as it merely takes into account precipitation (Gao et al., 2017). By contrast, standardized precipitation evapotranspiration index (SPEI) has been demonstrated as a comprehensive drought indicator that can accurately quantify regional drought intensity as it considers both precipitation and evapotranspiration (Vicente-Serrano et al., 2010). Therefore, SPEI was selected to quantify wet-dry environments and drought intensities among different agricultural districts. Determination for SPEI is based on the non-exceedance probability of the differences between precipitation and potential evapotranspiration (PET), reflecting deviation degree in drought or moist by standardizing the discrepancy between precipitation and PET. Obviously, the assessment of PET is essential, and it was performed using the Penman-Monteith model recommended by FAO (Allen et al., 1998). Differences between precipitation and *PET* were calculated at different time scales, which were normalized and standardized using a three-parameter log-Logistic probability distribution function that is capable of capturing the water deficit values (Vicente-Serrano et al., 2010). Compared

Table 1
Description and formula of landscape indicators.

Indicator	Interpretation	Formula
Number of patches (NP)	Amount of autocephalous landscape patch.	$NP = n_i$
Patch Richness (PR)	Number of different patch types present within landscape boundary.	$PR = q$
Patch Density (PD)	Number of patches divided by landscape area.	$PD = \frac{N}{A} \times 10000 \times 100$
Edge Density (ED)	Edge length per unit area.	$ED = \frac{E}{A} \times 10000$
Mean patch area (MEAR)	The average size of patches in a landscape.	$MEAR = \frac{\sum_{i=1}^{n}\sum_{j=1}^{m} a_{ij}}{N}$
Largest Patch Index (LPI %)	Proportion of the largest patch area to specific total landscape area.	$LPI = \frac{\max_{j=1}^{n} aij}{A} \times 100$
Percentage of Landscape (PLAND %)	Abundance percentage of a specific landscape category to overall landscape.	$PLAND = \frac{\sum_{j=1}^{n} a_{ij}}{A} \times 100$
Landscape Shape Index (LSI)	Morphological complexity of landscape patches.	$LSI = \frac{0.25 \times \sum_{k=1}^{m} e_{ik}}{\sqrt{A}}$
Fractal Dimension Index (FRAC)	Structure complexity of landscape patches.	$FRAC = \frac{2\ln(0.25p_{ij})}{\ln a_{ij}}$
Contiguity Index (CONTIG)	Spatial proximity and contiguity among landscape patches.	$CONTIG = \frac{\left[\frac{\sum_{r=1}^{z} c_{ijr}}{a_{ij}^{s}}\right] - 1}{v-1}$
Patch Cohesion Index (COHESION)	Physical connectedness, aggregation and landscape spatial pattern and characteristics.	$COHESION = \left[1 - \left(\frac{\sum_{i=1}^{n}\sum_{j=1}^{m} P_{ij}}{\sum_{i=1}^{n}\sum_{j=1}^{m} P_{ij} \times \sqrt{aij}}\right)\right] \times \left[1 - \left(\frac{1}{\sqrt{N}}\right)\right]^{-1} \times 100$
Contagion Index (CONTAG %)	A higher CONTAG for a given region indicates there is a preponderant landscape and a better clustering.	$CONTAG = \left[1 + \frac{\sum_{i=1}^{m}\sum_{k=1}^{m}\left[P_i \times \frac{g_{ik}}{\sum_{k=1}^{m} g_{ik}}\right] \times \left[\ln\left(P_i \times \frac{g_{ik}}{\sum_{k=1}^{m} g_{ik}}\right)\right]}{2\ln m}\right] \times 100$
Splitting Index (SPLIT)	Spatial separated and fragmentation extent between various landscape patches.	$SPLIT = \frac{A^2}{\sum_{i=1}^{m}\sum_{j=1}^{n} a_{ij}^2}$
Shannon's Diversity Index (SHDI)	Landscape diversification is proportional to land exploitation, a higher SHDI indicates a higher extent in land comprehensive development.	$SHDI = -\sum_{i=1}^{m}(P_i \times \ln P_i)$
Simpson's Diversity Index (SIDI)	Landscape diversity reflected by SIDI is less sensitive for infrequent landscape patches.	$SIDI = 1 - \sum_{i=1}^{m} P_i^2$

Note: E is boundary length for all patches in landscape (m); A is total landscape area (m^2); a_{ij} is area of patch ij (m^2); e_{ik} is edge length between patch types i and k; P_{ij} is perimeter of patch ij (m); C_{ijr} is contiguity for pixel r in patch ij; v is sum of values in a 3-by-3 cell template; a_{ij}^{s} is area of patch ij in terms of number of cells; m is number of landscape patch categories including landscape border; n is number of patch for a landscape; N is number of landscape patches; P_i is proportion of area of landscape patch type i in total landscape; q is number of patch types present in landscape excluding landscape border if present; g_{ik} is number of pixels adjacent to patch k within the landscape type i; g_{ii} is number of like adjacencies between pixels of patch type i based on the single-count method.

with two-parameter distribution, the three-parameter Log-logistic probability distribution provides an opportunity to address the inadequate consideration for some extreme negative values in water deficit for many arid and semi-arid regions (Tirivarombo et al., 2018). Detailed calculation is as the method of Vicente-Serrano et al. (2010). SPEI at scale of twelve months was selected to reflect dry-wet circumstances among different districts, because it can appropriately reflect dry-wet condition for a year.

2.5. Statistical analysis

Statistical analyses, including redundancy analysis, regression analysis and correlation analysis, were performed using SAS 9.4 and R 3.6.1 software.

3. Results

3.1. Spatiotemporal evolutions in landscape pattern at holistic landscape level for different national-level agricultural districts

Given that China is an important agricultural producer globally, the spatiotemporal changes in landscape pattern at the scale of national-level agricultural district were examined. There is a conspicuous spatial discrepancy in NP among different agricultural districts from 1980 to 2018, with a variation ranging from 51,677 to 189,935. The largest NP was recorded in NASR, followed by MLYP, YGP and SBSR. For PR, the discrepancy among various agricultural districts was not significant, and PR tended to increase first and then decrease during 1980—2018 for the vast majority of agricultural districts. Both PD and ED in SBSR, LP, MLYP, YGP and SC were higher than those in other districts. The values of MEAR in NASR, QTP and NCP were significantly higher than that in other districts. Except for QTP, the NP, PD, MEAR and ED in other agricultural zones has no dramatic change with time. The values of LPI have obvious spatial differentiation among different districts, with a distribution interval of 4.199–50.842. The LPI values in HHHP and SC were generally higher than those in other districts, and the LPI in QTP, LP, HHHP and MLYP showed conspicuous temporal variations. Higher LSI values were mainly observed in NASR, QTP, MLYP and YGP for the last decades. Spatiotemporal variations in both FRAC and COHESION across different agricultural districts were not obvious. The higher CONTAG values were mainly concentrated in NCP, NASR, HHHP and QTP, while higher CONTIG values were recorded in NASR and QTP. The SPLIT showed a strong spatiotemporal irregularity and heterogeneity across China from 1980 to 2018, with a fluctuation range of 3.853—237.269. The highest SPLIT was recorded in YGP, followed by LP and QTP. The SHDI and SIDI for the most agricultural districts showed a trend of increasing first and then decreasing (Fig. 2).

3.2. Dynamic variations in landscape pattern for different vegetation cover types

Landscape pattern indicators at subordinate class level were further examined to explore different categories of vegetation landscape dynamics (i.e. forest landscape, grass landscape and crop landscape). As a whole, the landscape pattern characteristics and dynamic evolutions of the three categories of vegetation among various national-level agricultural districts are quite different (Fig. 3).

For forest landscape, the highest annual average PLAND was presented in SC, reaching 62.26%; followed by YGP, with annual average value of 59.09%, indicating the higher forest abundance in these two agricultural districts. In addition, MLYP, NCP and SBSR also have a moderate percentage of forest landscape, with the annual average values of 46.69%, 44.37% and 34.83%, respectively. The minimum PLAND was recorded in NASR, with annual average value of merely 7.54%. Overall, there is significant discrepancy in abundance of forest landscape among different agricultural regions across China, reflecting the great heterogeneity in natural vegetation coverage among various regions. The discrepancy in LPI among nine agricultural districts was prominent. The highest LPI was recorded in YGP, followed by SC, MLYP and NCP, with the annual average values of 53.79%, 46.26%, 41.02% and 20.94%, respectively. The minimum LPI was recorded in QTP, with the annual average value of merely 3.72%. It is worth highlighting that the largest annual LPI in YGP is approximately 14.46 times the minimum LPI in QTP, manifesting a prominent discrepancy and spatial heterogeneity in forest landscape dominance among various agricultural districts. Similarly, higher forest MEAR values were

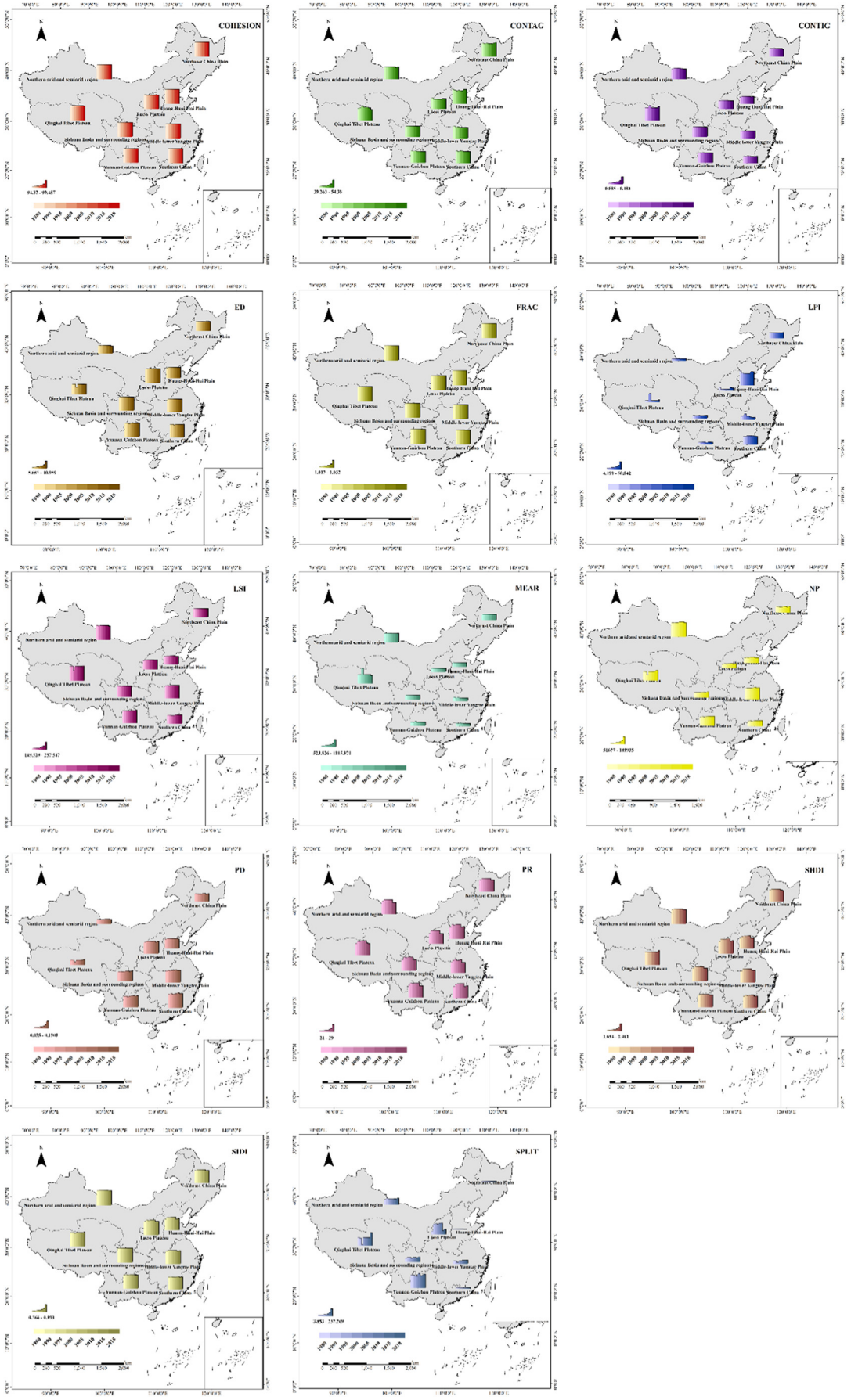

Fig. 2. Spatiotemporal variation in landscape pattern at holistic landscape level for different national-level agricultural districts.

also distributed in YGP, SC, MLYP and NCP, indicating a relatively higher forest landscape magnitude in these regions. On the contrary, agricultural districts with higher LPI and MEAR generally have a lower NP, such as YGP, SC and MLYP, while those with lower LPI and MEAR generally have a higher NP, such as NASR and QTP. This further confirmed that in regions with higher forest landscape dominance degree and larger forest planting scale, concentricity and continuity for forest landscape are usually stronger, and fragmentation degree of forest patches is relatively lower. During last nearly four decades, the highest annual average LSI was observed in YGP, reaching 177.94; followed by NASR and SBSR, with annual average LSI values of 171.37 and 166.21 respectively. The minimum LSI was observed in HHHP, with an annual mean value of 89.92, which is approximately 50% of the maximum LSI in YGP. Obviously, there is significant discrepancy in the complexity and irregularity of forest landscape structure among different agricultural districts. From 1980 to 2018, agricultural districts ranking in a descending order of annual average forest CONTIG are QTP, YGP, SC, NCP, SBSR, LP, MLYP, NASR and HHHP, respectively (Fig. 3a).

Grass landscape abundance in QTP has always been prominently higher than that in other districts, with annual fluctuation range of 49.66%—63.52% during 1980—2018. In addition, grass landscape in NASR, LP and SBSR also occupied an appropriate proportion in territorial holistic landscape, with annual variation ranges of 34.58%—37.66%, 33.90%—37.89% and 31.11%—32.68%, respectively. The lowest PLAND for grassland was recorded in MLYP, with an annual mean value of 3.71%. It is worth emphasizing that landscape dominance degree of grassland varied greatly among different regions during 1980—2018. Specifically, the highest LPI was recorded in QTP, followed by SBSR, with annual variation ranges of 34.10%—58.46% and 21.99%—23.46%, respectively. Meanwhile, the LPI of grassland in MLYP, NCP and SC has never exceeded 1% over last decades. Analogously, the largest MEAR has also been invariably recorded in QTP regardless of year, manifesting the absolute advantage in grass landscape of QTP among nine agricultural districts. It's worth noting that the number of grassland patches (NP) in QTP was not prominent in nine regions, while the NP of grass landscape in some regions with lower

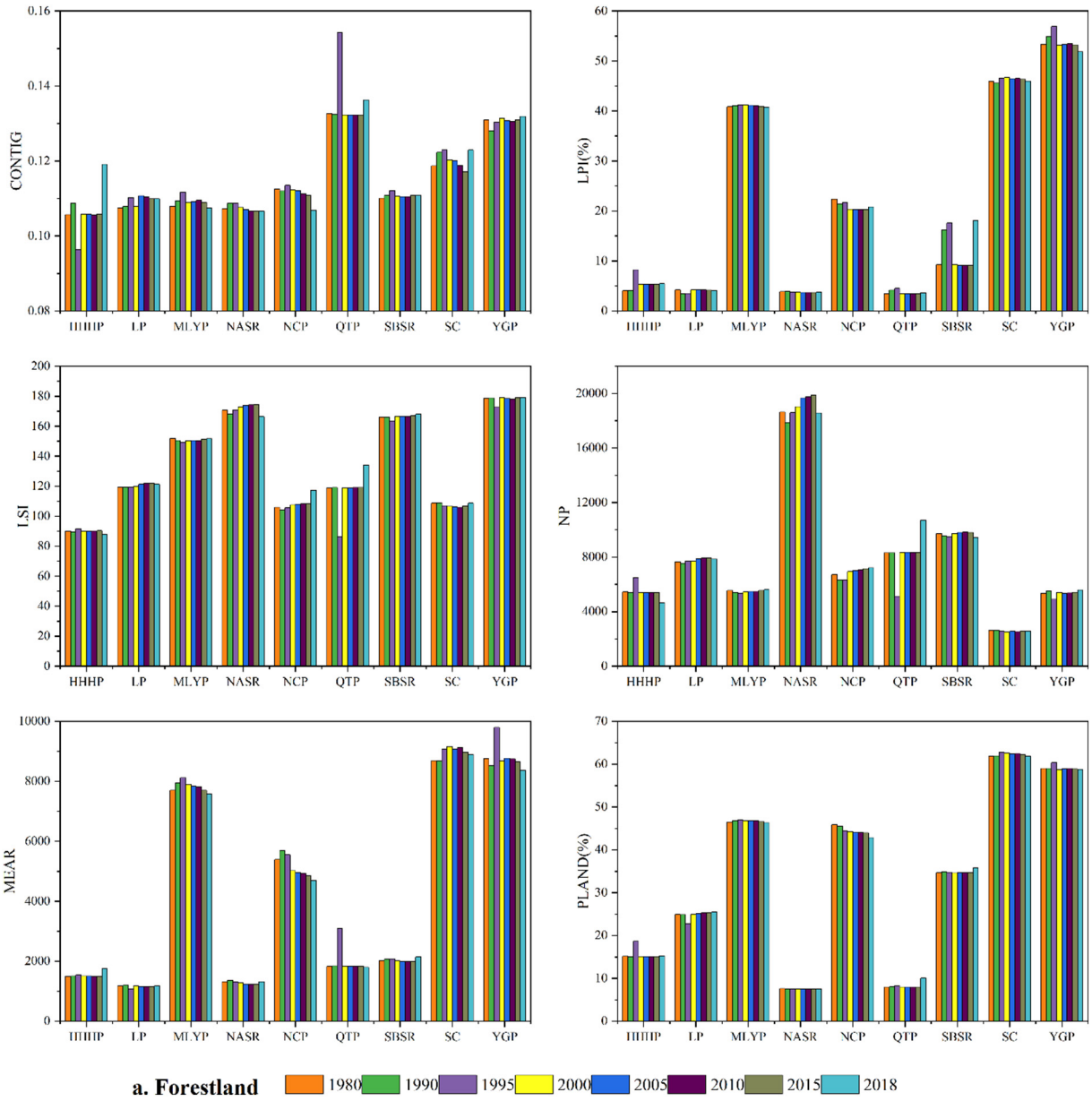

Fig. 3. Spatiotemporal variation in ecological landscape pattern of different vegetation cover categories at class level.

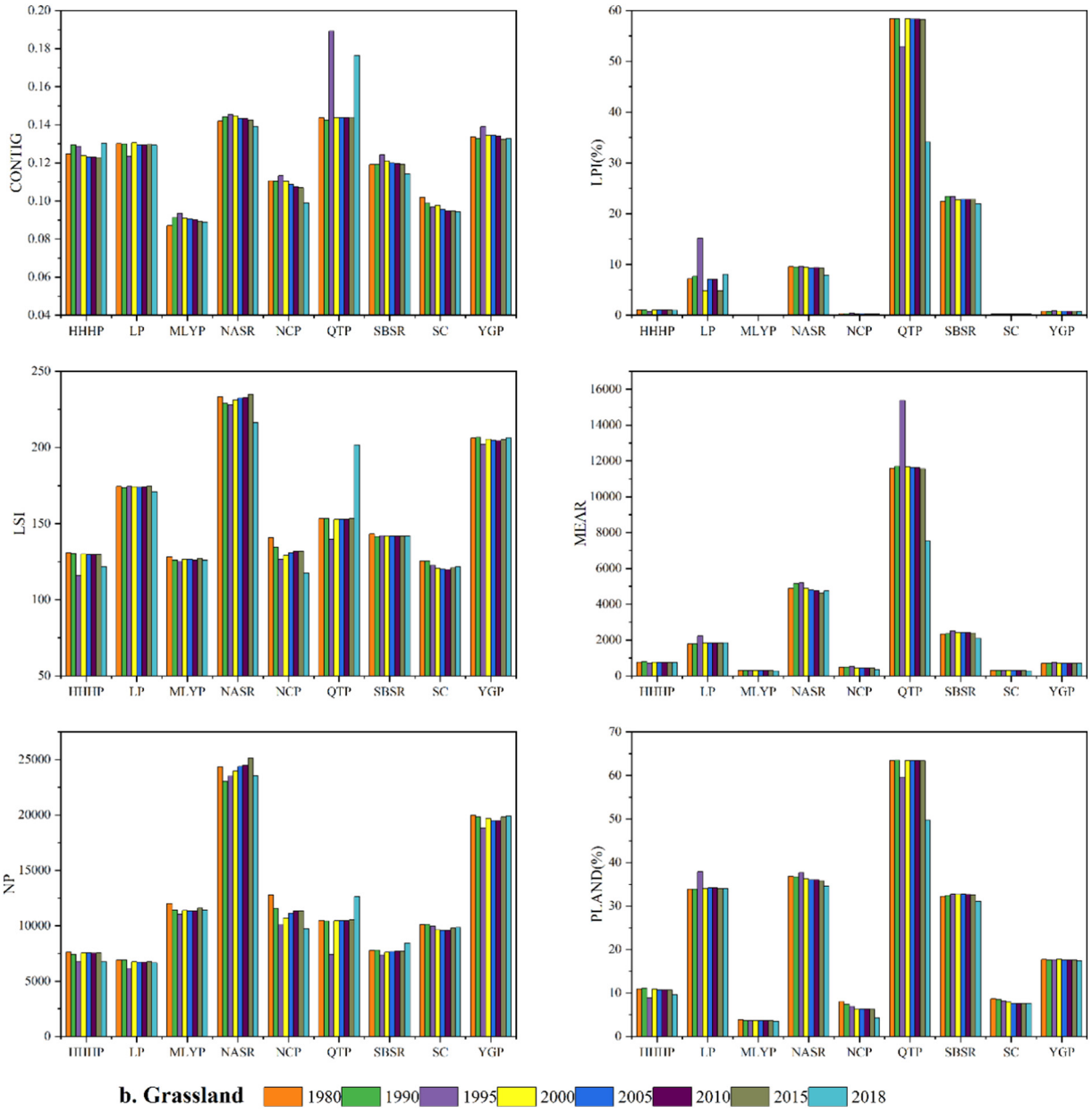

Fig. 3 (*continued*).

grassland dominance and abundance was relatively higher, such as YGP, NCP, SC, NASR and MLYP. This illustrates that grass landscape with a strong fragmentation and dispersion generally has lower landscape dominance. The nine agricultural regions can be ranked as NASR, YGP, LP, QTP, SBSR, NCP, HHHP, MLYP, SC, in descending order of LSI of grass landscape, with annual average LSI of 229.65, 205.14, 173.75, 157.53, 141.99, 130.39, 127.21, 126.53, 122.06, respectively. From 1980 to 2018, the largest LSI has always been presented in NASR, which is nearly twice that in SC. Such discrepancy indicates the complexity and irregularity of grass landscape structure varied greatly among different regions, which is related to the discrepancies in grassland management and greening policies between different districts. The highest grass landscape CONTIG occurred in QTP, followed by NASR and YGP, indicating a stronger spatial connectedness and contiguity of grassland in these districts (Fig. 3b).

During last nearly four decades, the HHHP has the largest proportion of crop landscape among several agricultural districts, with an annual mean PLAND of 59.15% and an annual PLAND fluctuating interval of 56.53%—60.64%. Moreover, crop landscape in MLYP, NCP and LP has also occupied a non-negligible proportion in regional holistic landscape, with annual average PLAND of 38.73%, 37.34%, 35.98%, and annual fluctuating range of 36.64%—40.17%, 33.63%—39.38%, 34.46%—36.74%, respectively. Abundance ratio of crop landscape in QTP was always the lowest from 1980 to 2018, with an annual average PLAND of merely 0.68%. Such discrepancy in crop landscape abundance suggests a great heterogeneity of agricultural development level among various agricultural districts across China. Furthermore, the maximum values of LPI and MEAR of cropland were also recorded in the HHHP, indicating the highest crop dominance and agricultural development scale in this region. Agricultural development degree varied greatly with agricultural district as results of the enormous discrepancies in both LPI and MEAR for crop landscape among different districts. Similar to forestland and grassland, a district with a lower LPI and MEAR for cropland usually has a higher NP, such as the YGP. This phenomenon indicates that the fragmentation and dispersion of any category of vegetation landscape, ordinarily, are inversely proportional

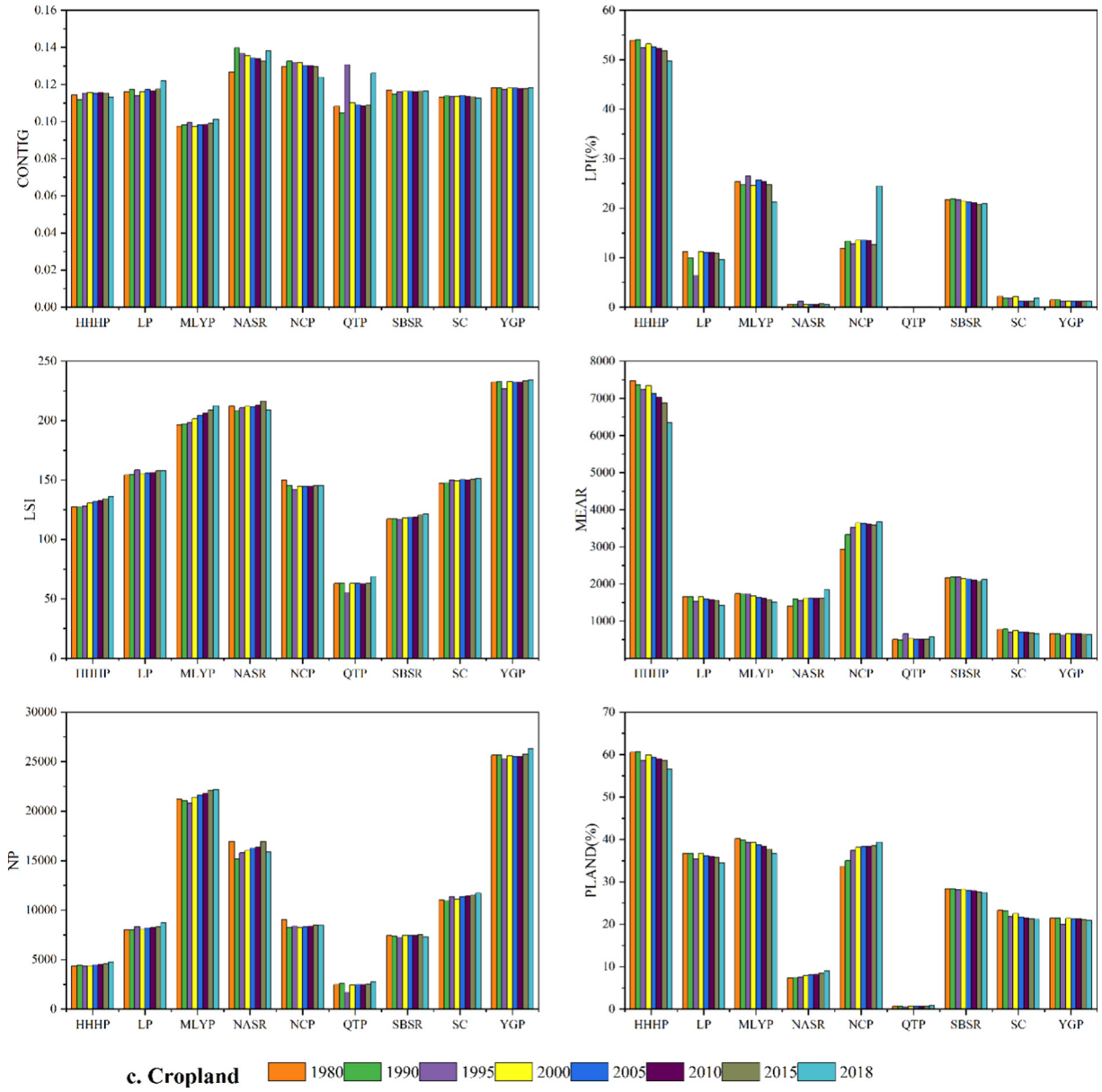

Fig. 3 (*continued*).

to the dominance and scale of that regardless of vegetation cover type. The nine agricultural districts can be ranked as YGP, NASR, MLYP, LP, SC, NCP, HHHP, SBSR and QTP, in descending order of LSI for crop landscape. Over last decades, the largest LSI has always been recorded in YGP, varying from 226.92 to 234.19, which are nearly 3—4 times that in QTP. During last decades, higher annual CONTIG for crop landscape mainly occurred in NASR and NCP, indicating a stronger spatial connectedness for cropland in these two districts. Compared with forestland and grassland, the difference of spatial connectivity for cropland between different agricultural districts was not noteworthy (Fig. 3c).

3.3. Spatial-temporal variation in dry-wet dynamics among different national-level agricultural districts

From 1980 to 2018, varying degrees of droughts have occurred in China's nine national-level agricultural districts. NASR and LP were always the most prominent two districts among all the agricultural districts across China in consideration of intensity and frequency in regional average dry-wet environment deterioration. Moreover, YGP, NCP and QTP have also showed a worsening tendency in regional dry-wet environment for particular years, such as YGP in 2005 and 2010, NCP in 2000 and QTP in 2015. For the vast majority of agricultural districts, regional average dry-wet levels have fluctuated greatly with time from 1980 to 2018. With the exception of 1990, the nine agricultural districts across China have more or less experienced varying extents of drought. Overall, there are significant discrepancies in dry-wet circumstances among different agricultural districts, and dry-wet dynamics across China have prominent spatiotemporal heterogeneity and uncertainty (Fig. 4a). To further examine the extreme drought intensities in disparate districts from 1980 to 2018, minimum SPEI for various agricultural districts were depicted in Fig. 4b. The most profound extreme drought intensity and frequency have uniformly presented within the QTP, in where prominent extreme drought conditions were recorded in 1980, 2010 and 2015, followed by the NASR in 1980 and 2005. Intense extreme droughts within the HHHP and LP have mainly occurred during 1995—2005. Among all agricultural districts, the MLYP has the lowest intensity and frequency of extreme drought. As a whole, occurrence, intensity and frequency of extreme drought have strong spatiotemporal uncertainty and heterogeneity across China's nine agricultural districts.

3.4. Correlations between landscape pattern at holistic landscape level and dry-wet dynamics

To systematically reveal the potential connections between ecological landscape variations and dry-wet dynamics during last decades, regression analysis between landscape variables and SPEI were conducted. Here, various landscape indicators, involving aspects of landscape patch density, abundance, shape, spatial distribution, structure characteristics and diversity, were selected for the regressions with SPEI, which is conducive to comprehend comprehensive influences of ecological landscape changes on dry-wet situations. Overall, correlation between regional holistic landscape pattern and dry-wet circumstance was obvious. There were varying degrees of positive correlations between average SPEI and PR, PD, LPI, LSI, COHESION, CONTAG. Inversely, average SPEI were negatively correlated with NP, MEAR, SPILT, SHDI, SIDI (Fig. 5). To further reveal the potential impact of landscape pattern variation on the intensity of extreme drought, regression analysis between landscape indicators and local minimum SPEI were performed. As a whole, landscape pattern indicators were observably correlated with minimum SPEI. Concretely, the minimum SPEI showed a downward trend with increasing NP, PR, MEAR, LSI, FRAC, SPLIT, SHDI and SIDI, while that exhibited an upward trend with increases in PD, ED, LPI and COHESION (Fig. 6). These indicate that regional holistic dry-wet dynamics and extreme drought intensity are related to the transformation direction of landscape pattern under influence of human activities. To some extent, landscape patch amount, density, configuration, structure, aggregation, connectivity and diversity could affect dry-wet balance and the intensity of extreme drought.

3.5. Influence of landscape pattern variation in different vegetation cover categories on dry-wet dynamics

To further reveal the potential relationship between landscape pattern of different vegetation category and dry-wet dynamics, correlation analysis between landscape variables at class level with SPEI was conducted respectively for forest, grass and crop landscape. Results showed that regional average SPEI was significantly positively correlated with COHESION of forest landscape and negatively correlated with LSI of Grass landscape ($p < 0.05$), suggesting the connectivity in forest landscape and the structural complexity in grass landscape would significantly associated with regional dry-wet dynamics. There was no obvious correlation between dry-wet dynamics and crop landscape pattern. It is worth highlighting that landscape pattern characteristics at vegetation (class) level were significantly related to the extreme drought intensity, regardless of vegetation category. Specifically, extreme drought intensity was prominently positively correlated with MEAR, LPI, PLAND and COHESION in forest and crop landscape, while it was prominently negatively correlated with MEAR, LPI, PLAND and COHESION in grass landscape. These results suggest that increased dominance, abundance, scale and spatial connectedness in forest and crop landscape may reduce the intensity of extreme drought in a particular district, but the opposite is true for grass landscape. In addition, there was significantly positive correlation between extreme drought intensity and NP only for forest landscape, and there was significantly negative correlation between extreme drought intensity and LSI only for crop landscape (Table 2).

3.6. Redundancy analysis (RDA) considered both landscape and vegetation levels comprehensively

Redundancy analysis (RDA) was further performed for synthetically comparing dry-wet dynamics with landscape pattern variables in both holistic landscape level and vegetation level, to determine the mutual correlations among various landscape variables, and to quantify their contributions to variance of dry-wet dynamics and extreme drought intensity. As a whole, the model demonstrated a significant influence of ecological landscape pattern on dry-wet dynamics. Canonical axis1 explained 38.53% of result variance and canonical Axis2 explained 25.74% of that. Red arrows represent ecological landscape indicators in landscape and class level respectively, and black arrows represent regional average SPEI and minimum SPEI. All the landscape variables associated with cropland and a large proportion of variables associated with forestland were positively correlated with the canonical axis1, while most landscape variables associated with grassland were negatively correlated with the canonical axis1. This implies the heterogeneity in ecological landscape characteristics between grass landscape and other two categories of vegetation landscape to some extent. Overall, the influences of landscape pattern variables on extreme drought intensity were more prominent than those on regional average dry-wet level. Specifically, LPI of holistic landscape, MEAR, LPI and PLAND of both crop and forest landscapes, were positively correlated with the minimum SPEI, significantly. COHESION of holistic landscape was significantly positively correlated with the average SPEI; while COHESION of forest landscape showed significantly positive correlation with average and minimum SPEI concurrently. The COHESION in crop landscape was significantly positively correlated with the minimum SPEI but not with the average SPEI. Of these, the PLAND of both forest and crop landscapes showed the strongest relationship with the minimum SPEI. Moreover, the MEAR, PLAND, COHESION, LPI and LSI of grass landscape were negatively correlated with the minimum SPEI significantly, while only the LSI of grass landscape has significant negative correlation with the average SPEI. Of these, the PLAND of grass landscape has the strongest negative correlation with the minimum SPEI, followed by MEAR and LPI. In addition, the LSI, MEAR and NP at holistic landscape level were also negatively correlated with the minimum SPEI. Overall, results of RDA, which considered comprehensive effects of different landscape scales, are consistent with the results of regression analysis at landscape level and the results of correlation analysis at class level, further verifying the relationship between ecological landscape pattern and dry-wet circumstance (Fig. 7).

4. Discussion

4.1. Landscape pattern for the nine agricultural districts in China

Landscape pattern is an integrated result of various human activities and ecological processes (Dadashpoor et al., 2019; Deng et al., 2009; Liu et al., 2021a, 2021b). It reflects the permutation and combination patterns of ecological landscape elements with various structures and configurations at different spatial scales (Wu and Hobbs, 2002). Determining for landscape pattern is the basis of understanding ecological landscape function and regional development dynamics (Liu et al., 2021a, 2021b; Sun et al., 2022; Wu, 2019). From 1980 to 2018, landscape patterns in different national-level agricultural districts across China had transformed to varying extents. The discrepancy in evolutions of landscape variables among different districts is mainly caused by unsynchronized developments in human society and ecosystem among different districts. Such heterogeneity is highly related to various policy orientations and inconsistent regional development layouts.

Over last decades, the abundance, dominance and scale of forest landscape in SC, YGP, MLYP and NCP were prominently higher than those in other districts, demonstrating a higher forest coverage and a superior forest ecological function service level in these four districts. Three of the four agricultural districts with high forest coverage are mainly concentrated in relatively humid areas of southern China, while the dominance and abundance of forest landscape are generally lower in the arid and semi-arid areas of northern China. Mountainous and hilly areas are widely distributed in southern China, with humid climate and abundant precipitation, resulting in a greater potential for forestry production and management in these districts (Gao et al., 2021; Xie et al., 2013; Yang et al., 2021). High-quality and extensive forest resources are essential for soil and water conservation in many mountainous and stormy basins in southern China, and can greatly reduce risk of siltation in rivers and reservoirs downstream of basins due to frequent floods (Chen et al., 2021; Yao et al., 2019). Synthesizing the factors of natural environment attribute and regional development strategy, local governments in southern China have generally attached great importance

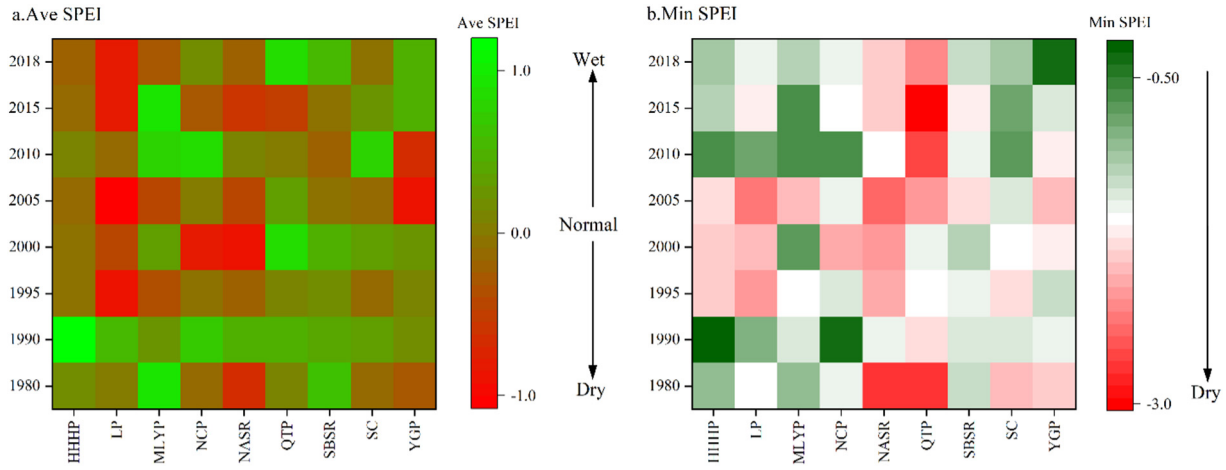

Fig. 4. Dry-wet dynamics among different national-level agricultural districts.

to the protection and construction of forest landscape. Such advantageous forest coverage has also contributed to the relatively higher level in ecological civilization construction in these regions. In addition, the abundance and dominance in forest landscape within the Northeast China Plain are more prominent among multiple regions of northern China, which is highly related to its physiographic characteristics and natural resource composition. Large-scale and widespread forestlands clustered in the Greater Khingan, Lesser Khingan and Changbai mountains within the NCP have been regarded as important natural forest areas in China (Tang et al., 2011; Yu et al., 2017; Zhang et al., 2021; Zhu and Lo, 2022). In these areas, natural forest resources and species are extremely abundant, contributing a non-negligible percentage of China's natural forest resources. It is worth highlighting that the vegetation landscape abundance and dominance examined in this study were based on landscape relative proportion at class level, rather than conventional absolute area analysis. Hence, the results of this research are more conducive to compare the vegetation landscape coverage and abundance between different regions as results of the normalized areas for various districts. It should be noted that the QTP has the highest forest landscape connectedness in spite of the lower forest abundance and dominance, which may be due to the strong spatial aggregation and reasonable landscape configuration of finite forest resources in this district. Structural complexity of forest landscape varied with agricultural district, which may be attribute to the disparate arrangement and combination of forest landscape among different districts as results of discrepancies in operation and management, terrain and slope characteristics, especially for natural forest areas. Among all agricultural districts, QTP has the highest grass landscape abundance and dominance, which is highly associated with its unique climatic characteristics and altitude. Cold climatic condition in this district has produced the largest alpine meadow vegetation area with the most abundant grass species and the widest grass resource distribution across China.

The most prominent abundance and dominance for crop landscape were presented in the HHHP as results of its absolute highest PLAND, LPI and MEAR in cropland, compared to other districts. The HHHP has always been the most momentous national grain production base and a representative agricultural area dominated by dry-farming, which produced approximately 50%—60% of China's wheat (Xiao and Tao, 2014; Zhang et al., 2013). Over last decades, the vast majority of primordial native vegetation in HHHP has been replaced by crops, thus crop landscape has become the dominating vegetation landscape type in this district. Although the coverage of crop landscape in HHHP was considerable, its morphological complexity and irregularity have been unspectacular, which should be attributed to the high-standard farmland construction, mature field mechanization operation, and intensive arable land management in HHHP. Although the abundance and dominance of crop landscape in YGP was relatively unremarkable, the number of autocephalous farmland patches has been identified as the highest among the nine districts, indicating the agricultural production pattern in this region is characterized by highly spatial decentralization. Such highly decentralized farmland management pattern may be related to the physical geographical characteristics of this district. Similarly, the highest spatial morphological complexity in crop landscape has always appeared in YGP, implying a relatively lower level in arable land planning and agricultural land management in this region. The reason may be that most of arable land resources in this region are generally operated by scattered individual farmers and minifundios, while there are few large-scale mechanized agricultural operation led by government. As a consequence, finite cultivated lands in YGP exhibited random, discrete and irregular landscape characteristics. Overall, there are significant discrepancies in landscape pattern between different vegetation types, and in holistic landscape and vegetation landscape characteristics between various districts.

It is worth emphasizing that variation characteristics in holistic landscape pattern and vegetation landscape pattern (class level) were disparate, suggesting the combination and interaction effects among various landscape elements are dependent on spatial scale. Spatially, different types of patch clusters generally present diverse distribution and combination types, such as random distribution, uniform distribution and aggregative distribution. Scale dependence of landscape pattern is mainly caused by discrepancies in landscape boundary transition zones, patch diversity, and combination mode of patch clusters. Accordingly, spatial scale effect should be considered primarily in landscape pattern optimization and configuration, as landscape structure would change with spatial scale, leading to a series of discrepancies and indeterminacies in ecosystem functions.

4.2. Potential impacts of landscape pattern on dry-wet circumstances

Droughts caused by extreme climate have seriously threatened the sustainable development in agriculture, social economy and ecological environment around the world, especially in arid and semi-arid regions (Dobler-Morales and Bocco, 2021; Mishra et al., 2021; Vicente-Serrano et al., 2020; Zhang et al., 2019). Response of extreme climate to land cover variation has attracted worldwide attention (Júnior et al., 2015; Peng et al., 2019). Transformation in land cover has a potential to trigger the change of various climatic factors, such as temperature, humidity and precipitation (Mahmood et al., 2014). Such effect occurs through changing a series of physical properties in land surface, and has significant spatial scale dependence (Betts et al., 2007). Considering that composition, distribution, morphology and configuration of land covers conjointly constitute landscape pattern, transformation in landscape pattern, hence, would inevitably affect dry-wet dynamics. As a whole, underlying correlations between landscape pattern and dry-wet dynamics were examined. Such

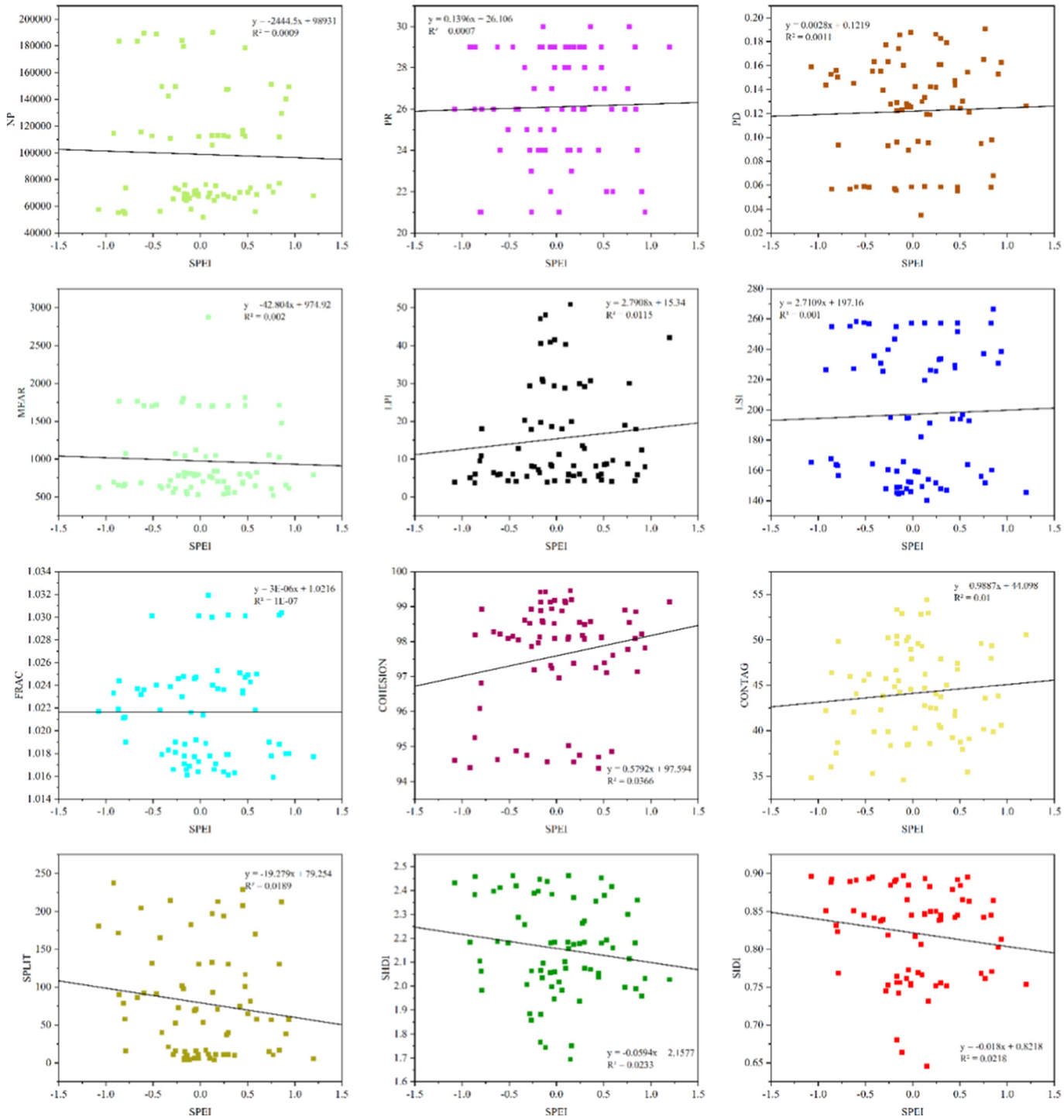

Fig. 5. Regression relationships between landscape pattern dynamics at holistic landscape level and mean dry-wet circumstances.

effect can be explained from following aspects: (1) Variation in landscape pattern will dramatically change a series of hydrological processes (Yohannes et al., 2021) such as vegetation evapotranspiration (Zhao et al., 2019) and surface runoff (Bin et al., 2018), as well as near-earth meteorological factors such as surface albedo, temperature and humidity (Gao et al., 2022; Shukla and Jain, 2021; Soydan, 2020), accordingly affecting dry-wet circumstances; (2) landscape pattern can regulate regional dry-wet balance through affecting geophysical characteristics (Ahmadi Mirghaed and Souri, 2022); and (3) transformation in landscape pattern will lead to variations in ecosystem function and service (Xia et al., 2021), thus impacting transmission and exchange of matter, energy and information, which may affect regional water transport and circulation and thus the dry-wet dynamics.

Results of redundancy analysis, regression analysis and correlation analysis have unanimously demonstrated that the potential contribution of landscape pattern to variability of extreme drought intensity was significantly higher than holistic dry-wet circumstance. Regional holistic dry-wet condition at national-level agricultural district scale would be improved with increases in dominant patch abundance and landscape connectedness. On the contrary, it will be deteriorated with increasing landscape fragmentation and diversity. It has been revealed that landscape pattern has the ecological potential to regulate local or regional climatic

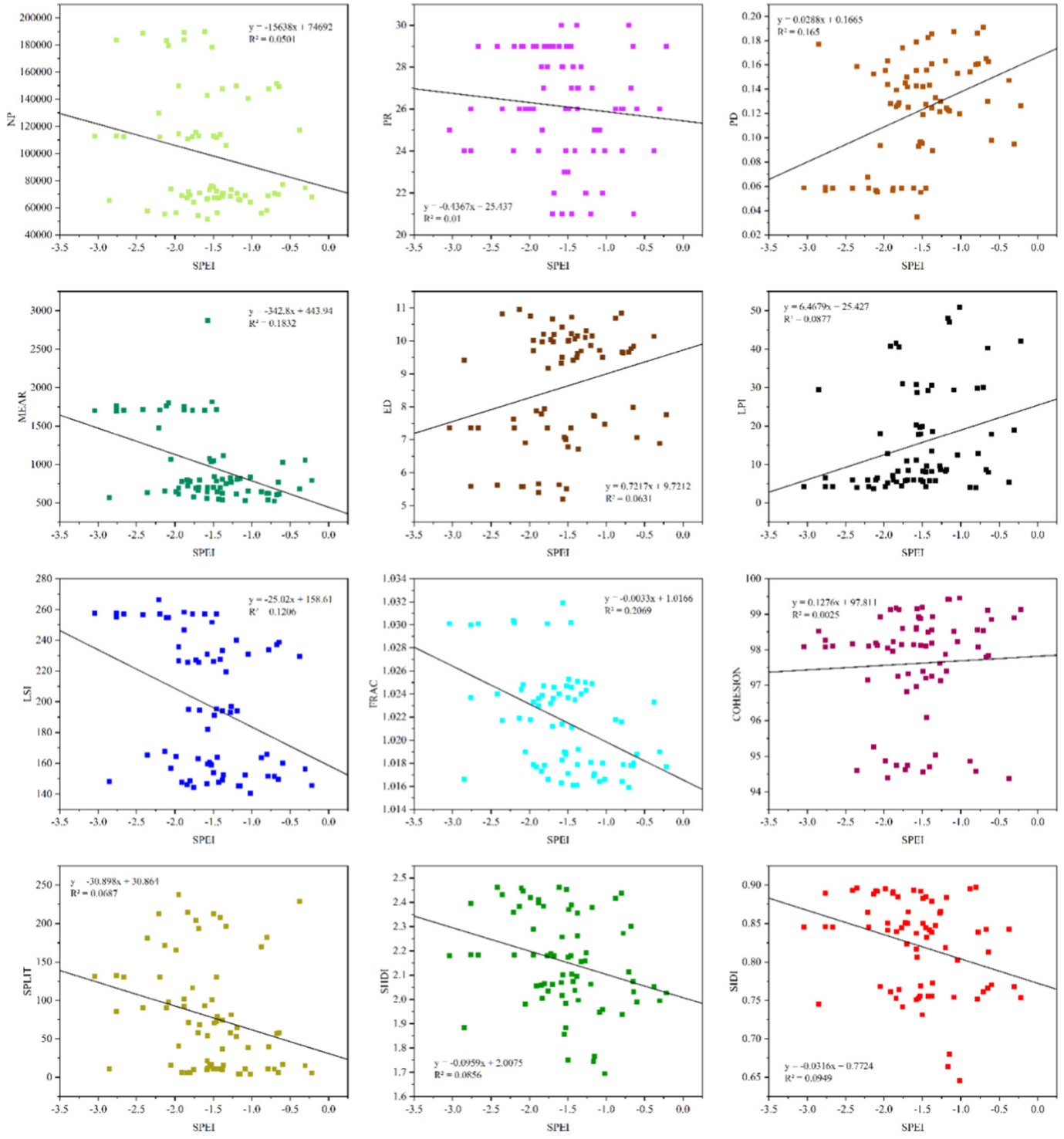

Fig. 6. Regression relationships between landscape pattern dynamics at holistic landscape level and extreme drought intensities.

circumstances through influencing surface albedo, land surface roughness and vegetation evapotranspiration (Peng et al., 2019; Perugini et al., 2017; Tayyebi et al., 2014). Nevertheless, specific mechanisms of influences of various elements in landscape pattern on dry-wet dynamics remain unclear. Increased diversity would contribute to the enhancement in function and service of ecosystem (Queiroz et al., 2015; Verhagen et al., 2016). In such a context, regional ecological diversity and corresponding water consumption tend to increase. Although a higher diversity in holistic landscape can be understood as a diversified and integrated progress of regional ecosystem, it also implies water consumption intensity caused by multiple industries may be intensified, thus aggravating drought. In this study, enhanced landscape connectivity showed a potential to improve regional dry-wet environment. The reason for this phenomenon may be that appropriate connectedness can promote the transfer and exchange of matter, energy and information between various ecological units (Oliveira-Junior et al., 2020; Zhao et al., 2019), thus enhancing ecosystem stability, and improving the capacity of circumvention and resistance against extreme disasters. Inversely, some landscapes with poor connectivity generally have higher surface albedo owing to large areas of bare land, such as gobi desert and sandy land. In where, intensive and continuous

Table 2
Correlation matrixes between landscape pattern indicators and SPEI for different vegetation cover categories.

Vegetation categories	Indicators	NP	MEAR	LPI	LSI	COHESION	PLAND	Ave. SPEI	Min. SPEI
Forest landscape	NP	1							
	MEAR	−0.605***	1						
	LPI	−0.571***	0.980***	1					
	LSI	0.497***	0.136	0.257*	1				
	COHESION	−0.207	0.775***	0.761***	0.331**	1			
	PLAND	−0.649***	0.907***	0.918***	0.129	0.684***	1		
	Ave. SPEI	−0.210	0.151	0.129	−0.066	0.236*	0.112	1	
	Min. SPEI	−0.361**	0.268*	0.265*	−0.121	0.241*	0.348**	0.601***	1
Grass landscape	NP	1							
	MEAR	0.097	1						
	LPI	−0.141	0.925***	1					
	LSI	0.806***	0.258*	0.060	1				
	COHESION	0.139	0.527***	0.516***	0.576***	1			
	PLAND	0.076	0.898***	0.886***	0.441**	0.751***	1		
	Ave. SPEI	−0.149	0.027	0.113	−0.291*	−0.190	−0.087	1	
	Min. SPEI	−0.221	−0.482***	−0.425**	−0.339**	−0.334**	−0.513***	0.601***	1
Crop landscape	NP	1							
	MEAR	−0.393**	1						
	LPI	−0.274*	0.895***	1					
	LSI	0.918***	−0.170	−0.148	1				
	COHESION	0.055	0.570***	0.610***	0.314**	1			
	PLAND	−0.098	0.796***	0.869***	0.077	0.726***	1		
	Ave. SPEI	−0.077	0.052	0.146	−0.213	−0.117	0.029	1	
	Min. SPEI	0.138	0.272*	0.359**	0.164	0.332**	0.476***	0.601***	1

* Significant at $p < 0.05$.
** Significant at $p < 0.01$.
*** Significant at $p < 0.0001$.

surface heat is usually more serious than other areas. Negative relationship between average wet-dry condition and landscape separation has further demonstrated this deduction. Landscape patches with different particle sizes may produce various ecological effects. For instance, a complete 100-square-meter green patch can contribute more cooling effects to land surface than 10 scattered 10-square-meter green patches (Li et al., 2017). Furthermore, the area of core zone for green landscape patch is the key element to improve local wetness. However, only the patch with a considerable large acreage has a core zone (Peng et al., 2019). Combining above two aspects, it seems not difficult to understand why an increase in dominant patch abundance tends to reduce regional drought risk. In addition, increased landscape edge density also has the potential to mitigate drought intensity. Change in landscape boundary may propose some impacts on local wet-dry states, as changing climates had been recorded along and near the boundaries of landscape transition and crossover (Mahmood et al., 2014). Increasing edge density may enhance the boundary transition zone between different landscape types, thus reducing boundary resistance, accordingly reducing the probability of local climate abrupt change.

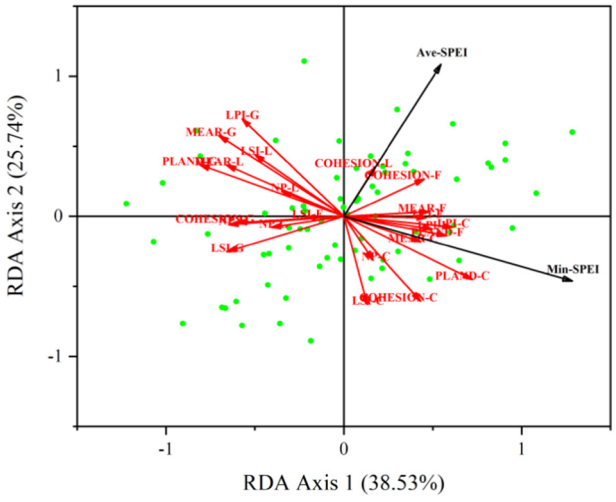

Fig. 7. Ordination of redundancy analysis (RDA) with dry-wet dynamics and landscape pattern variables. (Note: L represents synthesis landscape; F represents forestland; G represents grassland; C represents cropland).

At class level, the impacts and contributions of ecological landscape pattern of different vegetation types on regional dry-wet circumstances were quite disparate. Concretely, promotions in abundance, dominance and scale of forest and crop landscapes tended to reduce the intensity of extreme drought. Interestingly, the opposite was true for grass landscape. Such discrepancy should be related to the difference in photosynthesis and surface energy exchange process caused by the difference in natural properties and biological characteristics of different types of vegetation. For example, compared to grass, tree and crop are generally characterized by a higher height and leaf area index, which are more conducive to maintaining a humid climate environment in near-surface. Many studies have demonstrated that higher vegetation indices have the potential to reduce regional drought risk and to improve regional dry-wet condition. For instance, many positive relationships between vegetation indices (such as the normalized difference vegetation index (NDVI) and net primary production (NPP)) and a series of drought indices (such as the palmer drought severity index (PDSI), standard precipitation index (SPI) and standard precipitation evapotranspiration index (SPEI)) have been recorded in previous researches (Ji and Peters, 2003; Vicente-Serrano et al., 2013; Xu et al., 2012; Zhang and Zhang, 2019). Interaction mechanism between vegetation dynamics and wet-dry circumstances is complex, associating with multiple eco-physiological and environmental factors. Apart from influence of vegetation indices, species with deeper roots, such as tree and crop instead of grass, tend to be less vulnerable to the negative impacts of water deficit (Hanson and Weltzin, 2000; Zhang and Zhang, 2019). Thus, they usually have a higher potential in maintaining greater leaf coverage and sustained transpiration, thereby reducing land surface temperature and maintaining surface moisture, which is conducive to reduce the risk of extreme drought.

Previous research has revealed remarkable negative correlations between landscape metrics of forestland and drought intensity, but there was no obvious relationship between forest landscape variables and flood intensity (Peng et al., 2019), which is similar to our results. Our study found that the increases in forest landscape abundance, dominance, scale and connectivity have a possibility to significantly reduce the intensity of extreme drought, while only forest connectivity is significantly correlated

with regional mean dry-wet level. Many studies have illustrated that the intensity of evapotranspiration, photosynthesis and respiration of forest is usually stronger than that of other land cover categories owing to its considerable leaf coverage and greenness, which is more conducive to promoting regional hydrologic cycle and improving surface microclimate environment and soil water condition (Fan et al., 2015; Júnior et al., 2015; Peng et al., 2019; Serpa et al., 2015). Moreover, increased abundance of forest landscape may increase precipitation probability to some extent (Perugini et al., 2017), thus reducing the risk of extreme drought. A previous study has implied that the increase in core area of woodland might elevate the possibility of flood within a particular region (Peng et al., 2019). This also means that increased abundance and dominance of forest landscape can offer an opportunity to greatly reduce the risk of drought. Indeed, only a sizable patch has a core area, which makes it not hard to understand why the conspicuous correlation between LPI of forest landscape and extreme drought intensity was present. It is worth noting that enhancive spatial connectedness in forest landscape might significantly improve regional average dry-wet environment. The reason for this phenomenon may be that enhanced connectivity tends to facilitate the flow and circulate of water vapor within woodlands, improving vegetation photosynthetic and transpiration efficiency, reducing heat accumulation, thus improving climate condition and dry-wet circumstance in land surface.

Similar to forestland, the positive effects of increasing abundance and dominance in crop landscape on dry-wet environment are related to increased scale of transpiration and surface climate regulation effect. On the other hand, improved crop landscape connectivity may significantly promote water and heat circulation, and thus reducing heat cumulative effect in farmland. Compared with forestland and grassland, determining appropriate crop landscape to reduce drought risk is more complex because it should consider the balance between agricultural comprehensive economic benefits and ecological landscape effects involving varies cropping structures and crop categories.

In this study, the PLAND of grassland has contributed the most to extreme drought intensity, followed by MEAR and LPI. Compared with forestland and cropland, grassland has a lower efficacy to reduce surface temperature and maintain moisture, as results of its relatively weaker transpiration and lower evapotranspiration (Júnior et al., 2015; Perugini et al., 2017; Tayyebi et al., 2014). Geographically, large-scale open meadow in China is often distributed in some dry plateaus with little precipitation. Spacious grassland is often associated with strong xerothermic wind, which is easy to form atmospheric drought. The low height for grass results in a large total effective area receiving solar radiation and a high surface albedo. Finite moisture produced by grass transpiration is easily carried away by xerothermic wind after volatilizing into atmosphere. As a consequence, its capacity to retain water and humidity is significantly lower than forestland and cropland. Furthermore, increased spatial connectedness and structural complexity of grass landscape tend to aggravate drought risk and intensity. Enhancement in grassland connectivity would promote the circulation of water vapor and energy, which can accelerate the rate of water loss from grass transpiration driven by xerothermic wind at low altitude. Therefore, the arrangement and adjustment of landscape connectivity with the purpose of regulating dry-wet environment should be based on specific vegetation category, and various environmental factors such as vegetation attributes and physical geographical discrepancies should be took into account synthetically. Moreover, a patch with complex structure indicates a higher irregularity in surface morphology, which would result in a complicated surface albedo and radiation condition, and thus leading to an aggravating drought. Previous research has also suggested that degraded grassland with complicated structure and edge density is usually accompanied by a higher albedo, which is positively related with drought events (Peng et al., 2019). This conforms to present results.

4.3. Suggestions of suitable landscape optimization strategy

This research explored the correlation between ecological landscape pattern and dry-wet dynamics on a national scale for the first time. It offers a potential opportunity to regulate regional dry-wet circumstance by optimizing landscape configuration and construction. The results can provide a theoretical guidance and scientific basis for rational project and optimization of ecological landscape structure for the perspective of optimizing dry-wet condition and reducing drought risk. Some concrete suggestions can be proposed. In future landscape planning and land management practice, it is necessary to integrate isolated and scattered patches as much as possible, reducing landscape fragmentation and enhancing integrality, concentricity and continuity. For instance, reducing the amount of scattered unutilized lands, combining some fragmented and irregular small lands with their surrounding large-scale land covers, and promoting land intensive utilization and water and soil conservation projects are conducive to alleviate drought risk. Moreover, enhancing connectivity and reducing separation between patches are also conducive to reducing drought risk. For example, in many arid regions, unused bare lands can be converted into forestlands to enhance the connectivity of vegetation landscape, thus improving ecosystem function and stability, and ameliorating dry-wet environment. In the process of ecological landscape layout and optimization at class level, different categories of vegetation landscape should be optimized in different paths. For example, the concentrated abundance, dominance and spatial connectedness for forest landscape should be improved as much as possible under the premise of ensuring the coordinated development of regional multi-industries. On the premise of ensuring the basic ecological function and demand of grassland, the abundance proportion of grass landscape in the whole vegetation landscape should be appropriately weaken. Compared with forest and grass landscapes, deliberation of suitable crop landscape is more complex as it should dialectically consider the balance between agricultural integrated economic benefits and ecological landscape effects. In view of this, it is essential to explore the ecological landscape effects and economic benefits of different planting structures of various crops and their combinations in future.

This research has explored the potential relationship between terrestrial landscape pattern and wet-dry environment on a national scale for the first time. Nevertheless, there are still some scale limitations and potentially unexplained variables. Some environmental parameters (e.g. soil and elevation) are spatially heterogeneous and uncontrollable, which may contribute to some errors and uncertainty for present results, although they are difficult to avoid in large-scale regional studies. Given this, some long-term and small scale of factors-controlled field experiments need to be conducted to further examine and improve present results in future.

5. Conclusion

In this study, China was selected as the study region to examine the potential influence of ecological landscape pattern on dry-wet dynamic at national-level agricultural district scale.

From 1980 to 2018, landscape pattern among nine agricultural districts across China had transformed to varying extents and showed noteworthy spatiotemporal heterogeneity, which is mainly caused by unsynchronized progress in human activities and ecological environment for different districts. The abundance and dominance for forest landscape in SC, YGP, MLYP and NCP were higher than those in other districts. The QTP has the highest forest connectedness in spite of its lower abundance and dominance. Among all agricultural districts, QTP has the highest grass landscape abundance and dominance, which is associated with its climate and altitude. The most prominent crop landscape abundance and dominance were recorded in the HHHP as results of its absolute highest PLAND, LPI and MEAR in croplands. Although crop landscape abundance and dominance in YGP was unobtrusive, both patch number and structural complexity have been identified as the highest among nine districts, suggesting agricultural development pattern in YGP is characterized by highly decentralization. Overall, there are significant discrepancies in landscape indicators between various vegetation categories. The combination and interaction effects of various landscape variables are dependent on spatial scale, which should be considered in landscape configuration and optimization.

At holistic landscape level, dry-wet circumstance could be improved with the enhancement of the largest patch percentage, patch density and spatial connectivity, while worsen with the increase of landscape fragmentation and separated degree. Furthermore, increasing patch fragmentation and structure complexity may aggravate the intensity of extreme drought, while drought intensity may be alleviated with the increases of the largest patch percentage and edge density.

At class level, the contributions of vegetation landscape variables to dry-wet dynamics varied with vegetation category. Increases in abundance and dominance of forest and crop landscapes would reduce drought intensity and risk, while it was opposite for grass landscape. Improved forest connectedness would prominently optimize regional holistic dry-wet environment and reduce the risk of extreme drought. Among all landscape indicators, the PLAND of forest and crop landscapes contributed the most prominent effect to alleviate drought intensity. On the contrary, the PLAND of grassland showed the greatest contribution on exacerbating drought intensity. Moreover, increased spatial connectedness and morphological complexity of grass landscape tend to aggravate drought risk. Compared with forestland and grassland, determining suitable crop landscape configuration to reduce drought risk is more complex because the balance between agricultural integrated economic benefits and ecological landscape effects should be taken into account.

CRediT authorshop contribution statement

Yang Han: Viewpoint, Methodology, Conceptualization, Visualization, Writing.

Di Chang: Conceptualization, Visualization.

Xiao-zhi Xiang: Validation, Supervision, Material and financial support.

Jing-lei Wang: Validation, Supervision, Financial support.

All the authors have revised and examined the manuscript, and approved the manuscript.

Declaration of competing interest

The authors declare that they have no known competing financial interests or personal relationships that could have appeared to influence the work reported in this paper.

Acknowledgements

This work was jointly funded by the Natural Science Foundation of China (Grant No. 51879268), the Central Public-interest Scientific Institution Basal Research Fund (Grant No. FIRI20210105) and the Startup Foundation in Sichuan Normal University (KY20200901).

References

Aguilos, M., Sun, G., Noormets, A., Domec, J.C., McNulty, S., Gavazzi, M., Minick, K., Mitra, B., Prajapati, P., Yang, Y., King, J., 2021. Effects of land-use change and drought on decadal evapotranspiration and water balance of natural and managed forested wetlands along the southeastern US lower coastal plain. Agric. For. Meteorol. 303, 108381. https://doi.org/10.1016/j.agrformet.2021.108381.

Ahmadi Mirghaed, F., Souri, B., 2022. Spatial analysis of soil quality through landscape patterns in the Shoor River Basin,Southwestern Iran. CATENA 211, 106028. https://doi.org/10.1016/j.catena.2022.106028.

Allen, R.G., Pereira, L.S., Raes, D., 1998. Crop Evapotranspiration-Guidelines for Computing Crop Water Requirements-FAO Irrigation and Drainage. Food Agric. Organ. United Nations, Rome, Italy.

Asadi Zarch, M.A., Sivakumar, B., Sharma, A., 2015. Droughts in a warming climate: a global assessment of standardized precipitation index (SPI) and reconnaissance drought index (RDI). J. Hydrol. 526, 183–195. https://doi.org/10.1016/j.jhydrol.2014.09.071.

Betts, R.A., Falloon, P.D., Goldewijk, K.K., Ramankutty, N., 2007. Biogeophysical effects of land use on climate: model simulations of radiative forcing and large-scale temperature change. Agric. For. Meteorol. 142, 216–233. https://doi.org/10.1016/j.agrformet.2006.08.021.

Bin, L., Xu, K., Xu, X., Lian, J., Ma, C., 2018. Development of a landscape indicator to evaluate the effect of landscape pattern on surface runoff in the Haihe River Basin. J. Hydrol. 566, 546–557. https://doi.org/10.1016/j.jhydrol.2018.09.045.

Chen, J., Li, Z., Xiao, H., Ning, K., Tang, C., 2021. Effects of land use and land cover on soil erosion control in southern China: implications from a systematic quantitative review. J. Environ. Manag. 282, 111924. https://doi.org/10.1016/j.jenvman.2020.111924.

Dadashpoor, H., Azizi, P., Moghadasi, M., 2019. Land use change, urbanization, and change in landscape pattern in a metropolitan area. Sci. Total Environ. 655, 707–719. https://doi.org/10.1016/j.scitotenv.2018.11.267.

Deng, J.S., Wang, K., Hong, Y., Qi, J.G., 2009. Spatio-temporal dynamics and evolution of land use change and landscape pattern in response to rapid urbanization. Landsc. Urban Plan. 92, 187–198. https://doi.org/10.1016/j.landurbplan.2009.05.001.

Deng, X., Gibson, J., Wang, P., 2017. Relationship between landscape diversity and crop production: a case study in the Hebei Province of China based on multi-source data integration. J. Clean. Prod. 142, 985–992. https://doi.org/10.1016/j.jclepro.2016.03.174.

Ding, Y., Xu, J., Wang, X., Peng, X., Cai, H., 2020. Spatial and temporal effects of drought on Chinese vegetation under different coverage levels. Sci. Total Environ. 716, 137166. https://doi.org/10.1016/j.scitotenv.2020.137166.

Dobler-Morales, C., Bocco, G., 2021. Social and environmental dimensions of drought in Mexico: an integrative review. Int. J. Disaster Risk Reduct. 55, 102067. https://doi.org/10.1016/j.ijdrr.2021.102067.

Esfahanian, E., Nejadhashemi, A.P., Abouali, M., Adhikari, U., Zhang, Z., Daneshvar, F., Herman, M.R., 2017. Development and evaluation of a comprehensive drought index. J. Environ. Manag. 185, 31–43. https://doi.org/10.1016/j.jenvman.2016.10.050.

Fan, X.G., Ma, Z.G., Yang, Q., Han, Y.H., Mahmood, R., 2015. Land use/land cover changes and regional climate over the Loess Plateau during 2001–2009. Part II: interrelationship from observations. Clim. Chang. 129, 441–455. https://doi.org/10.1007/s10584-014-1068-5.

Gao, Xuerui, Zhao, Q., Zhao, X., Wu, P., Pan, W., Gao, Xiaodong, Sun, M., 2017. Temporal and spatial evolution of the standardized precipitation evapotranspiration index (SPEI) in the Loess Plateau under climate change from 2001 to 2050. Sci. Total Environ. 595, 191–200. https://doi.org/10.1016/j.scitotenv.2017.03.226.

Gao, X., Wang, G., Innes, J.L., Zhao, Y., Zhang, X., Zhang, D., Mi, F., 2021. Forest ecological security in China: a quantitive analysis of twenty five years. Glob. Ecol. Conserv. 32, e01821. https://doi.org/10.1016/j.gecco.2021.e01821.

Gao, J., Gong, J., Yang, J., Li, J., Li, S., 2022. Measuring spatial connectivity between patches of the heat source and sink (SCSS): a new index to quantify the heterogeneity impacts of landscape patterns on land surface temperature. Landsc. Urban Plan. 217, 104260. https://doi.org/10.1016/j.landurbplan.2021.104260.

Gebremeskel, G., Tang, Q., Sun, S., Huang, Z., Zhang, X., Liu, X., 2019. Droughts in East Africa: causes, impacts and resilience. Earth-Sci. Rev. 193, 146–161. https://doi.org/10.1016/j.earscirev.2019.04.015.

Guttman, N.B., 1998. Comparing the palmer drought index and the standardized precipitation index. Water Resour. Assoc. 34, 113–121. https://doi.org/10.1111/j.1752-1688.1998.tb05964.x.

Hanson, P.J., Weltzin, J.F., 2000. Drought disturbance from climate change: response of United States forests. Sci. Total Environ. 262, 205–220. https://doi.org/10.1016/S0048-9697(00)00523-4.

Ji, L., Peters, A.J., 2003. Assessing vegetation response to drought in the northern Great Plains using vegetation and drought indices. Remote Sens. Environ. 87, 85–98. https://doi.org/10.1016/S0034-4257(03)00174-3.

Jiang, T.L., Su, X.L., Singh, V.P., Zhang, G.X., 2021. A novel index for ecological drought monitoring based on ecological water deficit. Ecol. Indic. 129. https://doi.org/10.1016/j.ecolind.2021.107804.

Júnior, J.L.S., Tomasella, J., Rodriguez, D.A., 2015. Impacts of future climatic and land cover changes on the hydrological regime of the Madeira River basin. Clim. Chang. 129, 117–129. https://doi.org/10.1007/s10584-015-1338-x.

Karlsen, R.H., Bishop, K., Grabs, T., Ottosson-Löfvenius, M., Laudon, H., Seibert, J., 2019. The role of landscape properties, storage and evapotranspiration on variability in streamflow recessions in a boreal catchment. J. Hydrol. 570, 315–328. https://doi.org/10.1016/j.jhydrol.2018.12.065.

Kyatengerwa, C., Kim, D., Choi, M., 2020. A national-scale drought assessment in Uganda based on evapotranspiration deficits from the bouchet hypothesis. J. Hydrol. 580, 124348. https://doi.org/10.1016/j.jhydrol.2019.124348.

Li, W., Cao, Q., Lang, K., Wu, J., 2017. Linking potential heat source and sink to urban heat island: heterogeneous effects of landscape pattern on land surface temperature. Sci. Total Environ. 586, 457–465. https://doi.org/10.1016/j.scitotenv.2017.01.191.

Li, X., Fan, W., Wang, Lunche, Luo, M., Yao, R., Wang, S., Wang, Lizhe, 2021. Effect of urban expansion on atmospheric humidity in Beijing-Tianjin-Hebei urban agglomeration. Sci. Total Environ. 759, 144305. https://doi.org/10.1016/j.scitotenv.2020.144305.

Liu, C., Zhang, F., Carl Johnson, V., Duan, P., te Kung, H., 2021. Spatio-temporal variation of oasis landscape pattern in arid area: human or natural driving? Ecol. Indic. 125, 107495. https://doi.org/10.1016/j.ecolind.2021.107495.

Liu, H., Liu, Y., Wang, C., Zhao, W., Liu, S., 2021. Landscape pattern change simulations in Tibet based on the combination of the SSP-RCP scenarios. J. Environ. Manag. 292, 112783. https://doi.org/10.1016/j.jenvman.2021.112783.

Lu, J., Carbone, G.J., Gao, P., 2019. Mapping the agricultural drought based on the long-term AVHRR NDVI and North American Regional Reanalysis (NARR) in the United States, 1981–2013. Appl. Geogr. 104, 10–20. https://doi.org/10.1016/j.apgeog.2019.01.005.

Lu, Y., Cai, H., Jiang, T., Sun, S., Wang, Y., Zhao, J., Yu, X., Sun, J., 2019. Assessment of global drought propensity and its impacts on agricultural water use in future climate scenarios. Agric. For. Meteorol. 278, 107623. https://doi.org/10.1016/j.agrformet.2019.107623.

Ma, T., Liang, Y., Lau, M.K., Liu, B., Wu, M.M., He, H.S., 2021. Quantifying the relative importance of potential evapotranspiration and timescale selection in assessing extreme drought frequency in conterminous China. Atmos. Res. 263, 105797. https://doi.org/10.1016/j.atmosres.2021.105797.

Mahmood, R., Pielke, R.A., Hubbard, K.G., Niyogi, D., Dirmeyer, P.A., Mcalpine, C., Carleton, A.M., Hale, R., Gameda, S., Beltrán-Przekurat, A., Baker, B., Mcnider, R., Legates, D.R.,

Shepherd, M., Du, J., Blanken, P.D., Frauenfeld, O.W., Nair, U.S., Fall, S., 2014. Land cover changes and their biogeophysical effects on climate. Int. J. Climatol. 34, 929–953. https://doi.org/10.1002/joc.3736.

Medeiros, A., Fernandes, C., Gonçalves, J.F., Farinha-Marques, P., 2021. Research trends on integrative landscape assessment using indicators – a systematic review. Ecol. Indic. 129. https://doi.org/10.1016/j.ecolind.2021.107815.

Metzger, J.P., Villarreal-Rosas, J., Suárez-Castro, A.F., López-Cubillos, S., González-Chaves, A., Runting, R.K., Hohlenwerger, C., Rhodes, J.R., 2021. Considering landscape-level processes in ecosystem service assessments. Sci. Total Environ. 796. https://doi.org/10.1016/j.scitotenv.2021.149028.

Mishra, A.K., Singh, V.P., 2010. A review of drought concepts. J. Hydrol. 391, 202–216. https://doi.org/10.1016/j.jhydrol.2010.07.012.

Mishra, A., Alnahit, A., Campbell, B., 2021. Impact of land uses, drought, flood, wildfire, and cascading events on water quality and microbial communities: a review and analysis. J. Hydrol. 596, 125707. https://doi.org/10.1016/j.jhydrol.2020.125707.

Mohammad Harmay, N.S., Kim, D., Choi, M., 2021. Urban Heat Island associated with land use/land cover and climate variations in MelbourneAustralia. Sustain. Cities Soc. 69, 102861. https://doi.org/10.1016/j.scs.2021.102861.

Oliveira-Junior, N.D., Heringer, G., Bueno, M.L., Pontara, V., Meira-Neto, J.A.A., 2020. Prioritizing landscape connectivity of a tropical forest biodiversity hotspot in global change scenario. For. Ecol. Manag. 472, 118247. https://doi.org/10.1016/j.foreco.2020.118247.

Pedro-Monzonís, M., Solera, A., Ferrer, J., Estrela, T., Paredes-Arquiola, J., 2015. A review of water scarcity and drought indexes in water resources planning and management. J. Hydrol. 527, 482–493. https://doi.org/10.1016/j.jhydrol.2015.05.003.

Peng, Y., Wang, Q., Wang, H., Lin, Y., Song, J., Cui, T., Fan, M., 2019. Does landscape pattern influence the intensity of drought and flood? Ecol. Indic. 103, 173–181. https://doi.org/10.1016/j.ecolind.2019.04.007.

Perugini, L., Caporaso, L., Marconi, S., Cescatti, A., Quesada, B., de Noblet-Ducoudré, N., House, J.I., Arneth, A., 2017. Biophysical effects on temperature and precipitation due to land cover change. Environ. Res. Lett. 12, 53002. https://doi.org/10.1088/1748-9326/aa6b3f.

Queiroz, C., Meacham, M., Richter, K., Norström, A.V., Andersson, E., Norberg, J., Peterson, G., 2015. Mapping bundles of ecosystem services reveals distinct types of multifunctionality within a Swedish landscape. Ambio 44, 89–101. https://doi.org/10.1007/s13280-014-0601-0.

Serpa, D., Nunes, J.P., Santos, J., Sampaio, E., Jacinto, R., Veiga, S., Lima, J.C., Moreira, M., Corte-Real, J., Keizer, J.J., Abrantes, N., 2015. Impacts of climate and land use changes on the hydrological and erosion processes of two contrasting Mediterranean catchments. Sci. Total Environ. 538, 64–77. https://doi.org/10.1016/j.scitotenv.2015.08.033.

Shukla, A., Jain, K., 2021. Analyzing the impact of changing landscape pattern and dynamics on land surface temperature in Lucknow city,India. Urban For. Urban Green. 58, 126877. https://doi.org/10.1016/j.ufug.2020.126877.

Son, N.T., Chen, C.F., Chen, C.R., 2020. Urban expansion and its impacts on local temperature in San Salvador,El Salvador. Urban Clim. 32, 100617. https://doi.org/10.1016/j.uclim.2020.100617.

Song, Z., Xia, J., She, D., Li, L., Hu, C., Hong, S., 2021. Assessment of meteorological drought change in the 21st century based on CMIP6 multi-model ensemble projections over mainland China. J. Hydrol. 601, 126643. https://doi.org/10.1016/j.jhydrol.2021.126643.

Soydan, O., 2020. Effects of landscape composition and patterns on land surface temperature: urban heat island case study for Nigde,Turkey. Urban Clim. 34, 100688. https://doi.org/10.1016/j.uclim.2020.100688.

Spinoni, J., Naumann, G., Vogt, J., Barbosa, P., 2015a. European drought climatologies and trends based on a multi-indicator approach. Glob. Planet. Change 127, 50–57. https://doi.org/10.1016/j.gloplacha.2015.01.012.

Spinoni, J., Naumann, G., Vogt, J.V., Barbosa, P., 2015b. The biggest drought events in Europe from 1950 to 2012. J. Hydrol. Reg. Stud. 3, 509–524. https://doi.org/10.1016/j.ejrh.2015.01.001.

Spinoni, J., Barbosa, P., De Jager, A., McCormick, N., Naumann, G., Vogt, J.V., Magni, D., Masante, D., Mazzeschi, M., 2019. A new global database of meteorological drought events from 1951 to 2016. J. Hydrol. Reg. Stud. 22, 100593. https://doi.org/10.1016/j.ejrh.2019.100593.

Sun, X., Yang, P., Tao, Y., Bian, H., 2022. Improving ecosystem services supply provides insights for sustainable landscape planning: a case study in Beijing,China. Sci. Total Environ. 802, 149849. https://doi.org/10.1016/j.scitotenv.2021.149849.

Tang, L.N., Li, A.X., Shao, G.F., 2011. Landscape-level forest ecosystem conservation on Changbai Mountain, China and North Korea (DPRK). Mt. Res. Dev. 31, 169–175. https://doi.org/10.1659/MRD-JOURNAL-D-10-00120.1.

Tayyebi, A., Pijanowski, B.C., Linderman, M., Gratton, C., 2014. Comparing three global parametric and local non-parametric models to simulate land use change in diverse areas of the world. Environ. Model. Softw. 59, 202–221. https://doi.org/10.1016/j.envsoft.2014.05.022.

Teuling, A.J., Van Loon, A.F., Seneviratne, S.I., Lehner, I., Aubinet, M., Heinesch, B., Bernhofer, C., Grunwald, T., Prasse, H., Spank, U., 2013. Evapotranspiration amplifies European summer drought. Geophys. Res. Lett. 40, 2071–2075. https://doi.org/10.1002/grl.50495.

Tirivarombo, S., Osupile, D., Eliasson, P., 2018. Drought monitoring and analysis: standardised precipitation evapotranspiration index (SPEI) and standardised precipitation index (SPI). Phys. Chem. Earth 106, 1–10. https://doi.org/10.1016/j.pce.2018.07.001.

Tordoni, E., Casolo, V., Bacaro, G., Martini, F., Rossi, A., Boscutti, F., 2020. Climate and landscape heterogeneity drive spatial pattern of endemic plant diversity within local hotspots in South-Eastern Alps. Perspect. Plant Ecol. Evol. Syst. 43, 125512. https://doi.org/10.1016/j.ppees.2020.125512.

Verhagen, W., Van Teeffelen, A.J.A., Baggio Compagnucci, A., Poggio, L., Gimona, A., Verburg, P.H., 2016. Effects of landscape configuration on mapping ecosystem service capacity: a review of evidence and a case study in Scotland. Landsc. Ecol. 31, 1457–1479. https://doi.org/10.1007/s10980-016-0345-2.

Vicente-Serrano, S.M., Beguería, S., López-Moreno, J., 2010. A multiscalar drought index sensitive to global warming: the standardized precipitation evapotranspiration index. J. Clim. 23, 1696–1718. https://doi.org/10.1175/2009JCLI2909.1.

Vicente-Serrano, S.M., Gouveia, C., Camarero, J.J., Begueria, S., Trigo, R., Lopez-Moreno, J.I., Azorin-Molina, C., Pasho, E., Lorenzo-Lacruz, J., Revuelto, J., Moran-Tejeda, E., Sanchez-Lorenzo, A., 2013. Response of vegetation to drought time-scales across global land biomes. Proc. Natl. Acad. Sci. U. S. A. 110, 52–57. https://doi.org/10.1073/pnas.1207068110.

Vicente-Serrano, S.M., Van der Schrier, G., Beguería, S., Azorin-Molina, C., Lopez-Moreno, J.I., 2015. Contribution of precipitation and reference evapotranspiration to drought indices under different climates. J. Hydrol. 526, 42–54. https://doi.org/10.1016/j.jhydrol.2014.11.025.

Vicente-Serrano, S.M., Quiring, S.M., Peña-Gallardo, M., Yuan, S., Domínguez-Castro, F., 2020. A review of environmental droughts: increased risk under global warming? Earth-Sci. Rev. 201, 102953. https://doi.org/10.1016/j.earscirev.2019.102953.

Wanders, N., Wada, Y., 2015. Human and climate impacts on the 21st century hydrological drought. J. Hydrol. 526, 208–220. https://doi.org/10.1016/j.jhydrol.2014.10.047.

Wang, Z., Li, J., Lai, C., Zeng, Z., Zhong, R., Chen, X., Zhou, X., Wang, M., 2017. Does drought in China show a significant decreasing trend from 1961 to 2009? Sci. Total Environ. 579, 314–324. https://doi.org/10.1016/j.scitotenv.2016.11.098.

Wang, L., Yu, H., Yang, M., Yang, R., Gao, R., Wang, Y., 2019. A drought index: the standardized precipitation evapotranspiration runoff index. J. Hydrol. 571, 651–668. https://doi.org/10.1016/j.jhydrol.2019.02.023.

Wang, T., Tu, X., Singh, V.P., Chen, X., Lin, K., 2021. Global data assessment and analysis of drought characteristics based on CMIP6. J. Hydrol. 596, 126091. https://doi.org/10.1016/j.jhydrol.2021.126091.

Wu, J.G., 2019. Linking landscape, land system and design approaches to achieve sustainability. J. Land Use Sci. 14, 173–189. https://doi.org/10.1080/1747423X.2019.1602677.

Wu, J.G., Hobbs, R., 2002. Key issues and research priorities in landscape ecology: an idiosyncratic synthesis. Landsc. Ecol. 17, 355–365. https://doi.org/10.1023/A:1020561630963.

Xia, H., Kong, W., Zhou, G., Sun, O.J., 2021. Impacts of landscape patterns on water-related ecosystem services under natural restoration in Liaohe River Reserve,China. Sci. Total Environ. 792, 148290. https://doi.org/10.1016/j.scitotenv.2021.148290.

Xiao, D., Tao, F., 2014. Contributions of cultivars, management and climate change to winter wheat yield in the North China Plain in the past three decades. Eur. J. Agron. 52, 112–122. https://doi.org/10.1016/j.eja.2013.09.020.

Xie, Y., Wen, Y., Zhang, Y., Li, X., 2013. Impact of property rights reform on household forest management investment: an empirical study of southern China. For. Policy Econ. 34, 73–78. https://doi.org/10.1016/j.forpol.2012.12.002.

Xu, J., Ren, L.L., Ruan, X.H., Liu, X.F., Yuan, F., 2012. Development of a physically based PDSI and its application for assessing the vegetation response to drought in northern China. J. Geophys. Res. 117. https://doi.org/10.1029/2011JD016807.

Xu, K., Yang, D., Yang, H., Li, Z., Qin, Y., Shen, Y., 2015. Spatio-temporal variation of drought in China during 1961–2012: a climatic perspective. J. Hydrol. 526, 253–264. https://doi.org/10.1016/j.jhydrol.2014.09.047.

Yang, M., Mou, Y., Meng, Y., Liu, S., Peng, C., Zhou, X., 2020. Modeling the effects of precipitation and temperature patterns on agricultural drought in China from 1949 to 2015. Sci. Total Environ. 711, 135139. https://doi.org/10.1016/j.scitotenv.2019.135139.

Yang, X., Liu, B., Bussmann, R.W., Guan, X., Xu, W., Xue, T., Xia, C., Li, J., Jiang, H., Wu, L., Yu, S., 2021. Integrated plant diversity hotspots and long-term stable conservation strategies in the unique karst area of southern China under global climate change. For. Ecol. Manag. 498, 119540. https://doi.org/10.1016/j.foreco.2021.119540.

Yao, N., Li, Y., Li, N., Yang, D., Ayantobo, O.O., 2018. Bias correction of precipitation data and its effects on aridity and drought assessment in China over 1961–2015. Sci. Total Environ. 639, 1015–1027. https://doi.org/10.1016/j.scitotenv.2018.05.243.

Yao, X., Yu, K., Wang, G., Deng, Y., Lai, Z., Chen, Y., Jiang, Y., Liu, J., 2019. Effects of soil erosion and reforestation on soil respiration, organic carbon and nitrogen stocks in an eroded area of Southern China. Sci. Total Environ. 683, 98–108. https://doi.org/10.1016/j.scitotenv.2019.05.221.

Yao, N., Li, L., Feng, P., Feng, H., Li Liu, D., Liu, Y., Jiang, K., Hu, X., Li, Y., 2020. Projections of drought characteristics in China based on a standardized precipitation and evapotranspiration index and multiple GCMs. Sci. Total Environ. 704, 1–18. https://doi.org/10.1016/j.scitotenv.2019.135245.

Yohannes, H., Soromessa, T., Argaw, M., Dewan, A., 2021. Impact of landscape pattern changes on hydrological ecosystem services in the Beressa watershed of the Blue Nile Basin in Ethiopia. Sci. Total Environ. 793, 148559. https://doi.org/10.1016/j.scitotenv.2021.148559.

Yu, L.X., Liu, T.X., Bu, K., Yang, J.C., Zhang, S.W., 2017. Monitoring forest disturbance in lesser Khingan mountains using MODIS and Landsat TM time series from 2000 to 2011. J. Indian Soc. Remote Sens. 45, 837–845. https://doi.org/10.1007/s12524-016-0645-7.

Zhang, X., Zhang, B., 2019. The responses of natural vegetation dynamics to drought during the growing season across China. J. Hydrol. 574, 706–714. https://doi.org/10.1016/j.jhydrol.2019.04.084.

Zhang, X., Wang, S., Sun, H., Chen, S., Shao, L., Liu, X., 2013. Contribution of cultivar, fertilizer and weather to yield variation of winter wheat over three decades: a case study in the North China Plain. Eur. J. Agron. 50, 52–59. https://doi.org/10.1016/j.eja.2013.05.005.

Zhang, X., Chen, N., Sheng, H., Ip, C., Yang, L., Chen, Y., Sang, Z., Tadesse, T., Lim, T.P.Y., Rajabifard, A., Bueti, C., Zeng, L., Wardlow, B., Wang, S., Tang, S., Xiong, Z., Li, D., Niyogi, D., 2019. Urban drought challenge to 2030 sustainable development goals. Sci. Total Environ. 693, 133536. https://doi.org/10.1016/j.scitotenv.2019.07.342.

Zhang, J.Q., Shen, X.J., Wang, Y.J., Jiang, M., Lu, X.G., 2021. Effects of Forest changes on summer surface temperature in Changbai Mountain,China. Forests 12. https://doi.org/10.3390/f12111551.

Zhao, X., Wei, H., Liang, S.L., Zhou, T., He, B., Tang, B.J., Wu, D.H., 2015. Responses of natural vegetation to different stages of extreme drought during 2009–2010 in Southwestern China. Remote Sens. 7, 14039–14054. https://doi.org/10.3390/rs71014039.

Zhao, F., Li, H., Li, C., Cai, Y., Wang, X., Liu, Q., 2019. Analyzing the influence of landscape pattern change on ecological water requirements in an arid/semiarid region of China. J. Hydrol. 578, 124098. https://doi.org/10.1016/j.jhydrol.2019.124098.

Zhou, H., Zhou, W., Liu, Yuanbo, Yuan, Y., Huang, J., Liu, Yongwei, 2020. Identifying spatial extent of meteorological droughts: an examination over a humid region. J. Hydrol. 591, 125505. https://doi.org/10.1016/j.jhydrol.2020.125505.

Zhu, L., Lo, K., 2022. Eco-socialism and the political ecology of forest conservation in the Greater Khingan Range, China. Polit. Geogr. 93, 102533. https://doi.org/10.1016/j.polgeo.2021.102533.

Zhu, Y., Liu, Yi, Wang, W., Singh, V.P., Ren, L., 2021. A global perspective on the probability of propagation of drought: from meteorological to soil moisture. J. Hydrol. 603, 126907. https://doi.org/10.1016/j.jhydrol.2021.126907.